EUR 5046 e

COMMISSION OF THE EUROPEAN COMMUNITIES

PULSED NEUTRONS AND THEIR UTILIZATION

by

W. KLEY

1974

Joint Nuclear Research Centre
Ispra Establishment - Italy

LEGAL NOTICE

This report is on sale at the addresses listed on cover page 4

at the price of B.Fr. 100.—

Commission of the
European Communities
D.G. XIII - C.I.D.
29, rue Aldringen
L u x e m b o u r g

February 1974

EUR 5046 e

PULSED NEUTRONS AND THEIR UTILIZATION by W. KLEY

Commission of the European Communities
Joint Nuclear Research Centre - Ispra Establishment (Italy)
Luxembourg, February 1974 - 74 Pages - 36 Figures - B.Fr. 100.—

General Considerations on the basic design elements of a periodically pulsed fast neutron source as core-geometry, moderator-geometry and material composition as well as operational data, pulse frequency, pulse shape, and background problems are forwarded and their benefits in detail discussed.

The design criteria for high resolution time of flight spectrometers for coherent and incoherent elastic and inelastic scattering experiments are enumerated. It is shown that also for time of flight spectroscopy the focusing condition can be fulfilled in general and that constant $\vec{\varkappa}$ as well as constant $\hbar\omega$-scans can be obtained from a two-dimensional time of flight analysis.

EUR 5046 e

PULSED NEUTRONS AND THEIR UTILIZATION by W. KLEY

Commission of the European Communities
Joint Nuclear Research Centre - Ispra Establishment (Italy)
Luxembourg, February 1974 - 74 Pages - 36 Figures - B.Fr. 100.—

General Considerations on the basic design elements of a periodically pulsed fast neutron source as core-geometry, moderator-geometry and material composition as well as operational data, pulse frequency, pulse shape, and background problems are forwarded and their benefits in detail discussed.

The design criteria for high resolution time of flight spectrometers for coherent and incoherent elastic and inelastic scattering experiments are enumerated. It is shown that also for time of flight spectroscopy the focusing condition can be fulfilled in general and that constant $\vec{\varkappa}$ as well as constant $\hbar\omega$-scans can be obtained from a two-dimensional time of flight analysis.

EUR 5046 e

PULSED NEUTRONS AND THEIR UTILIZATION by W. KLEY

Commission of the European Communities
Joint Nuclear Research Centre - Ispra Establishment (Italy)
Luxembourg, February 1974 - 74 Pages - 36 Figures - B.Fr. 100.—

General Considerations on the basic design elements of a periodically pulsed fast neutron source as core-geometry, moderator-geometry and material composition as well as operational data, pulse frequency, pulse shape, and background problems are forwarded and their benefits in detail discussed.

The design criteria for high resolution time of flight spectrometers for coherent and incoherent elastic and inelastic scattering experiments are enumerated. It is shown that also for time of flight spectroscopy the focusing condition can be fulfilled in general and that constant $\vec{\varkappa}$ as well as constant $\hbar\omega$-scans can be obtained from a two-dimensional time of flight analysis.

EUR 5046 e

COMMISSION OF THE EUROPEAN COMMUNITIES

PULSED NEUTRONS AND THEIR UTILIZATION

by

W. KLEY

1974

Joint Nuclear Research Centre
Ispra Establishment - Italy

Lectures held on the 5th Meeting on Magnetism and Neutron Physics at Gaussig, Dresden, Germany
November 13-17th, 1972

ABSTRACT

General Considerations on the basic design elements of a periodically pulsed fast neutron source as core-geometry, moderator-geometry and material composition as well as operational data, pulse frequency, pulse shape, and background problems are forwarded and their benefits in detail discussed.

The design criteria for high resolution time of flight spectrometers for coherent and incoherent elastic and inelastic scattering experiments are enumerated. It is shown that also for time of flight spectroscopy the focusing condition can be fulfilled in general and that constant $\vec{\varkappa}$ as well as constant $\hbar\omega$-scans can be obtained from a two-dimensional time of flight analysis.

KEYWORDS

MEETINGS
RESOLUTION
TIME-OF-FLIGHT SPECTROMETERS
COHERENT SCATTERING
ELASTIC SCATTERING
INELASTIC SCATTERING
INCOHERENT SCATTERING
NEUTRONS
PULSED NEUTRON TECHNIQUES
HF BR REACTOR
PULSED REACTORS
SPECIFICATIONS
REACTOR CORES
MODERATORS
NUCLEAR STRUCTURES
DATA
COMPARATIVE EVALUATIONS

Lecture I

General aspects important for the comparison and choice of a continuous, a periodically pulsed reactor and a periodically pulsed booster and General Considerations concerning the basic design elements for a periodically pulsed neutron source.

Lecture II

High resolution time of flight spectrometry at a pulsed neutron source.

Contents

Lecture I

Lecture II

I. Introduction

Neutrons have no charge and free neutrons have a finite life time $\tau = (11.7 \pm 0.3)$ min, thus even ultra-cold neutrons ($\vartheta \leq 5$ m/sec) can only be stored in neutron bottles for a limited time. Therefore free neutrons have to be produced continuously by nuclear reactions. A number of well-known reactions are used such as

(α, n), (γ, n), (p, n), (d, n),

the fission process, the spallation process and the fusion reaction. The production of neutrons is accompanied by the release of more or less heat depending on the nuclear reaction which is used and for a given production rate a corresponding cooling power has to be provided. For some reactions the heat release per neutron is given in Tab. 1.

Tab. 1

Reaction	Heat in MeV/neutron
1. $Be^9(d, n)B^{10}$ (d: 15 MeV)	1200
2. (γ, n) (e^-: 35 MeV)	2000
3. Fission-Process	100
4. Spallation Process	40
5. Fusion-Reaction $/T\ (d, n/He^4/$	17

From Tab. 1 one can see that in the first two reactions much more heat has to be removed from the production area. For all physics experiments not only the production rate is of importance, but also the neutron density which is proportional to the cooling power density.

Because of the short range of 15 MeV deuterons and of 35 MeV electrons (some mm) in the corresponding target material, the power density is especially high in the first two reactions of Tab. 1. These reactions have been used primarily for pulsed neutron sources (accelerator) with very high neutron peak flux within short time intervals $10^{-10} \leq \Delta t \leq$ some μsec and low

mean neutron yield. All neutron scattering experiments in which the momentum and energy transfer have to be determined, require not only a high neutron peak flux, but also a high mean neutron yield. Therefore neither the first two nor the last two reactions from Tab. 1 can be used for the construction of intense neutron sources. Steady state reactors, periodically pulsed reactors and periodically pulsed boosters will be in the next future (probably 20 years) the best neutron source for large mean neutron yield and also high neutron peak flux. The general aspects which favour a continuous high flux beam reactor (H. F. B. R.), a periodically pulsed fast reactor (P. P. F. R.) and a periodically pulsed fast booster (P. P. F. B.) are many and very different ones and they do not depend so much on technical and scientific arguments and the scientific program related with the neutron source but rather on political intentions and constellations.

II. General Aspects Important for the Comparison of the Benefits of a H. F. B. R., a P. P. F. R. and a P. P. F. B.

II. 1. The Heavy Water High Flux Beam Reactor (H. F. B. R.)

Without any doubt, the H. F. B. R. [1, 2, 3] with a thermal neutron flux $\Phi = 10^{15}$ n/cm^2. sec is the best neutron source for all experiments which require a high reaction rate as e. g. the production of transuranium elements, fission-product-beams, thermal neutron (n,γ) reactions and in general for all experiments that do not require a definition of the neutron energy. The H. F. B. R. has a compact undermoderated D_2O-cooled core and the thermal neutron peak reaches its peak value in the D_2O-moderator 15 cm away from the core. Fig. 1 shows a cross section of the Grenoble H. F. B. R. The reactor is suitable for the installation of a hot and cold neutron moderator, but the related technical and financial efforts are considerable. In Fig. 2, 3 and 4 the theoretical differential neutron flux values for the different neutron sources of the H. F. B. R. Grenoble are reproduced together with the flux values of the SORA-P. P. F. R. at an average power of 1 MWatt and an operation frequency of 50 cycles/sec.

The H. F. B. R. -Grenoble produces at a power of 55 MWatt and at a maximum power density of 3.3 MWatt/liter a thermal neutron flux of $\Phi = 1.10^{15}$ $n/cm^2 . sec$. With these values one reaches a barrier for the D_2O-water technology as well as in fuel cost which will not be pushed further since also it can be demonstrated that all experiments which require a determination of the momentum- and energy-transfer, thus all experiments concerning the static and dynamic structure of condensed matter, can be performed with a P. P. F. R. and a P. P. F. B. From present day technology it can already be expected that a P. P. F. R. with an average power of 30-50 MWatt can be designed and constructed after sufficient operational experience has been collected with a P. P. F. R. of some MWatt.

II. 2. The Periodically Pulsed Fast Reactor (P. P. F. R.)

The first not for destructive purpose developed pulsed fast reactors have been built in Los Alamos [4, 5, 6, 7]. They have been used to determine the different delayed neutron groups and their decay constants of the fission products of U^{235} and Pu^{239}. The so-called "burst reactors" have still a great importance for the dosimetry in biological systems as well as for the study of the transient phenomena in Radiation-Damage-Processes in semi-conductors and electronic circuits that are used in the most different technical installations.

The first periodically pulsed fast reactor has been put in operation at the Joint Institute for Nuclear Research at Dubna, U. S. S. R., in 1960. Fig. 5 shows the principle components. Under the influence of this event the first studies on a P. P. F. R. of high power have been initiated by V. Raievski at the end of 1961 at Ispra in Italy. These studies have been terminated now [11-19]. In two years from now the start-up of a 4 MWatt P. P. F. R., the so-called I. B. R. -II, is expected and some times later a linear electron accelerator of 200 kWatt power will be coupled to the I. B. R. -II for the P. P. F. B. -operation condition [20-21]. From Fig. 2, 3 and 4 it can be seen that a P. P. F. R. of the SORA-type (average power 1 MWatt and pulse

frequency ν = 50 cycles/sec) generates a cold neutron peak flux equivalent to the H. F. B. R. - Grenoble, a thermal neutron peak flux 1. 5 times higher, a hot neutron flux 4 times higher at 200 meV and an epithermal flux 10 times higher at E = 1 eV than the corresponding values of the H. F. B. R. Grenoble.

It is supposed that after a certain time ($\approx$ 1 year) the operation frequency can be lowered to 5 cycles/sec in favour of a 10-times higher peak flux at the same average power.

The P. P. F. R. with variable frequency has the potential to vary the fission rate or the neutron peak flux by one order of magnitude at the same average power level. Due to this characteristic property one cannot define a simple criteria as e. g. the maximum thermal neutron peak flux since the intensity of a scattering experiment is not determined alone by the maximum obtainable peak flux, but rather by the maximum obtainable time integrated (= stationary) flux.

If one is interested in a scientific valid comparison of a H. F. B. R. with a P. P. F. R. of the SORA-type, one has to examine case by case and one may not eliminate at will any given possibilities in order to arrive at an objective judgement of the situation. In my second lecture on the application of periodically pulsed fast neutron sources this problem will be investigated in more detail.

A P. P. F. R. of the SORA-type has a stationary fast neutron flux (identical with the time averaged fast flux) that is comparable with the H. F. B. R. Grenoble, but has a γ-heating value 30 times lower than the H. F. B. R., a very important fact for all low temperature radiation damage studies.

For the investigations of time dependent radiation damage phenomena, the application of noise analysis methods will improve the sensitivity by several orders of magnitude compared to the conventional continuous methods of resistance measurements. For similar motives the P. P. F. R. is a good instrument for the production of fission fragment beams induced by fast neutron fis-

sion alone. Fission fragment beams are used for the investigation of the fast fission process, the correlated $\beta^{\pm}$ emitters as well as delayed neutron emitters. Furthermore a P. P. F. R. can be used for the determination of group cross sections in the energy range of keV till some MeV; such data have a certain importance for the optimalization of fast breeders.

A P. P. F. R. of the SORA type is comparable or even better than a H. F. B. R. for all neutron scattering experiments that require a determination of the momentum- and energy-transfer, hence for all studies concerning the static and dynamic structure of condensed matter. For all experiments under extreme conditions (pulsed magnetic and electric fields, high pressure and high and low temperature) the low frequency P. P. F. R. ($\nu \leq 5$ cycles/sec) is a unique instrument and largely superior to a H. F. B. R. of the Grenoble type.

The installation of a cold neutron source in a P. P. F. R. of the SORA type is a rather simple enterprise, since the fast neutron flux and the γ-heating are very low at the position of the liquid para-hydrogen. A cooling power of about 20 Watt is required.

The construction of a P. P. F. R. of the SORA type is a necessary step to relieve the H. F. B. R. Grenoble from experiments that can be done either as well or even better with a P. P. F. R. and increase correspondingly the access to intense neutron sources and to obtain the necessary information concerning the behaviour of the different parts of the reactor under periodic pulsed conditions in order to provide the basis for the design of a P. P. F. R. of an average power of 50 MWatt or more.

II. 3. The Periodically Pulsed Fast Booster (P. P. F. B.)

H. Rief [22] has performed extensive time dependent Monte Carlo calculations for the differential neutron flux values for the different SORA-Moderator-configurations, as proposed by the author [23]. The time dependent differential neutron flux leaking from the moderator into the beam tubes

has been calculated for a $\delta(t)$ pulse of fast neutrons (SORA-spectrum) impinging on the moderator. This method allows not only to determine the peak flux values, but also the pulse shape and the effective neutron burst width which has been determined as the square root of the variance σ^2 of the neutron pulse $\Phi(t)$. The pulse half width values for the SORA-reactor have been obtained by folding the moderator $\delta(t)$-response pulse with the SORA power pulse. The moderator $\delta(t)$-response pulses for the different moderator configurations reflect already very well what kind of pulses one can expect for the case of the P. P. F. B.

The most important results are summarized in Tab. 2.

Tab. 2

Characteristic SORA-Moderator Data for P. P. F. R. and P. P. F. B. - operation condition [22]

Table 2.a

H_2O-Moderator [20x30x5] cm^3 T = 300°K	Reactor $\Delta\Theta$ = 65 µsec				Booster $\Delta\Theta$ = 7 µsec				Gain-Factors	
Energy-Interval	Φ_R	σ_R	$\bar{\Phi}_R$	$M_R \cdot 10^3$	Φ_B	σ_B	$\bar{\Phi}_B$	$M_B \cdot 10^3$	$\bar{\Phi}_G$	M_G ( )
3-10	0.02	89	1.78	0.225	0.05	33	1.65	1.51	0.925	6.7
10-30	0.22	89	19.6	2.47	0.50	33	16.5	15.1	0.84	6.1
30-110	0.58	86	50	6.75	1.29	32	41.3	40	0.825	5.91
110-230	0.18	80	14.4	2.25	0.96	9	8.65	107	0.60	47.5
3-230	1.00				2.80					
230-430	0.10	67	6.7	1.5	0.8	8	6.4	100	0.955	66.5
430-1000	0.12	65	7.8	1.85	1.1	7	7.7	157	0.98	85

Definitions:

$\Phi_G = \Phi_B / \Phi_R$, Energy : E [MeV], Moderator-Pulse-Half Width: σ [µ sec]

Definitions (contd.):

$M_G = M_B/M_R$

Power-Pulse-Half Width: $\Delta\Theta$ [μ sec]

Integrated Flux: $\bar{\Phi} \simeq \Phi \cdot \sigma$ [n/cm^2]

Peak Flux : Φ [n /cm^{2}sec]

Figure of merit: $M(\sigma) = \Phi/\sigma$ [n/cm^{2}sec^2]

Table 2.b

ZrH_2-Moderator /20x30x5/ cm^3 T = 700°K	Reactor $\Delta\Theta$ = 65 μsec				Booster $\Delta\Theta$ = 7 μ sec				Gain-Factors	
Energy-Interval	Φ_R	σ_R	$\bar{\Phi}_R$	$M_R \cdot 10^3$	Φ_B	σ_B	$\bar{\Phi}_B$	$M_B \cdot 10^3$	$\bar{\Phi}_G$	$M_G(\sigma)$
3-10										
10-30	0.06	89	5.35	0.675	0.15	37	5.55	4.05	1.03	6.0
30-100	0.43	82	35.2	5.24	1.04	33	34.5	31.5	0.98	6.0
100-220	0.51	81	41.3	6.30	1.25	30	37.5	41.7	0.91	6.6
3-220	1.00				2.44					
220-470	0.25	80	20	3.12	1.12	9	10	124	0.5	40
470-1000	0.14	66	9.25	2.12	1.11	7	7.8	159	0.84	75

Table 2.c

H_2O-H_2-Moderator *)	Reactor $\Delta\Theta$ = 65 μsec				Booster $\Delta\Theta$ = 7μsec				Gain-Factors	
Energy-Interval	Φ_R	σ_R	$\bar{\Phi}_R$	$M_R \cdot 10^3$	Φ_B	σ_B	$\bar{\Phi}_B$	$M_B \cdot 10^3$	$\bar{\Phi}_G$	$M_G(\sigma)$
1-3	0.10	105	10.5	9.5	0.19	80	15.2	2.38	1.45	0.25
3-10	0.32	105	33.6	3.05	0.46	65	30	7.1	0.90	2.3
10-30	0.34	105	35.7	3.23	0.54	60	32.4	9.0	0.91	2.8
30-110	0.15	84	12.6	1.79	0.46	22	10.1	20.9	0.80	11.7
110-230	0.09	68	6.9	1.32	0.45	12	5.4	37.5	0.78	28.5
1-230	1.00				2.10					
230-430	0.09	66	5.95	1.36	0.64	9.4	6.0	68	1.01	50

*) H_2O-Moderator [20x30x5] cm^3, T = 300°K
H_2 -Moderator [20x30x2] cm^3, T = 20°K

In this context the optimalization studies by G. Riccobono, V. Ardente and G. Rossi [24] are of importance. As we show later, there are reasons to define two optimalization parameters for experiments with pulsed neutron sources:

$$(1) \quad \bar{\Phi} = \int_{\text{pulse}} \Phi(E,t)dt = \left\{ \int_{\text{pulse}} \Phi_1(t)dt \right\} \cdot \Phi_2(E)$$

$$(2) \quad M(\sigma) = \frac{\int_{\text{pulse}} \Phi_1(t)dt}{\sigma^2} \approx \frac{\Phi_1^{\max}\left[\sigma(d)\right]}{\sigma(d)}$$

where $\Phi(E,t) = \Phi_1(t) \cdot \Phi_2(E)$, "d" the moderator thickness and $\sigma^2(d)$ the variance of $\Phi_1(t)$.

The following quantities

(3) $\overline{\Phi}_G = \overline{\Phi}_B / \overline{\Phi}_R$

(4) $M_G(\sigma) = M_B(\sigma) / M_R(\sigma)$

will therefore characterize the benefits of the P. P. F. B. compared to the P. P. F. R. From Table 2 and Fig. 6, 7 and 8 one can conclude that for scattering experiments with cold neutrons the P. P. F. B. has no advantages compared to the P. P. F. R. For thermal neutrons a gain factor = 6 and for the region of the hot neutrons a gain factor $M_G(\sigma) = 50$ can be obtained.

For cold and thermal neutron scattering experiments $M_G(\sigma)$, characterizing the intensity of a neutron scattering experiment, can still be increased on the expense of momentum transfer (K)-resolution. For this purpose the moderators are poisoned since the peak flux is much less influenced than σ, the moderator pulse half width. σ can be varied almost by one order of magnitude since the thermalization time of neutrons in H_2O-water is about 5 μsec and therefore neutron pulses with a duration of some μ sec can be produced in the total spectral region below 1 eV. For thermal neutrons it is estimated that the $M_G(\sigma)$-value can be improved from 6 to about 20. All experiments with a predetermined $d\Omega$ for which Φ is the optimalization parameter will lose intensity correspondingly. Respecting the constant power condition

$$\Phi_B^f \cdot \Delta t_B^f \cdot \nu_B = \Phi_R^f \cdot \Delta t_R^f \cdot \nu_R$$

where B and R stand for Booster and Reactor, "f" for the fast neutrons leaking from the core into the moderators and assuming equal pulse frequency $\nu_B = \nu_R$, one can increase the fast neutron peak flux by one order of magnitude by setting $\Delta t_B^f = \Delta t_R^f / 10$. For all fast neutron transmission experiments the gain factor $M_G = 100$ and experiments concerning time dependent phenomena in radiation damage processes will improve or be possible at all. As it can be seen from Tab. 2, the M_G values for hot and thermal neutrons are considerably smaller even by poisoning the moderators. For any neutron scattering experiment with a predetermined $d\eta$ or $\vec{K}$-resolution, the energy-transfer-resolution can be improved on the expense of intensity. For time

of flight experiments the intensity will be at most proportional to $/\Delta\hbar\omega/\hbar\omega/^2$ and not proportional to $/\Delta\hbar\omega/\hbar\omega/^3$ as for conventional triple axis spectrometer. In this respect one has to see the benefits of a P. P. F. B. compared to a P. P. F. R.

III. Reasons that Lead to the Definition of Two Moderator Optimalization Parameters: $\bar{\tau}$ and $M(\sigma)$

Fig. 9, 10 and 11 /22/ show the stationary epithermal, thermal and cold neutron flux at the surface and in the center of moderators of various thickness "d". The stationary neutron flux $\Phi = \int \Phi(E,t)\,dt$ reaches its maximum in the center of the moderator, therefore the moderators have to have a thickness of about 10-12 cm and reentrant holes should make partially the $\bar{\tau}$ accessible to the experiments. This procedure leads to a rather long relaxation time τ for the different neutron sources that is given approximately by:

$$(5) \qquad \tau \simeq \frac{1}{\bar{v}} \cdot \frac{1}{D.B^2 + \Sigma_a}$$

where $\bar{v}$ stands for the average neutron velocity, D for the average neutron diffusion constant, Σ_a for the average macroscopic absorption constant and B^2 for the buckling or the geometry of the moderator. For the moderators in the SORA-Reactor one obtains $\tau \geq \Delta t_R^f$ the neutron pulse characteristic is therefore entirely determined by the moderator property and geometry. For a maximum $\bar{\tau}$ value one obtains therefore $\Delta t_M \approx 120\ \mu$ sec. Because of this rather long pulse duration, long flight paths have to be used for the thermal and cold neutron experiments with an energy resolution between

$$(6) \qquad 1^o/_{oo} \lesssim \frac{1}{2}\,\frac{\Delta E}{E} = \frac{\Delta t_M}{t} = \frac{\sigma}{l} \cdot \vartheta \lesssim \text{some } \%$$

For any neutron scattering experiment the neutron current density at the position of the target is given by:

$$(7)\quad I(E)dE = \frac{1}{4\pi}\left\{\int_{\text{pulse}} \Phi\ (E,t)dt\right\} dE\ d\Omega.\ \nu\left[n/cm^2.sec\right]$$

$$= \frac{1}{4\pi}\left\{\int_{\text{pulse}} \Phi_1(t)dt\right\}.\Phi_2(E).dE.d\Omega.\nu$$

where $\Phi(E,t) = \Phi_1(t).\ \Phi_2(E)$, $d\Omega = F_Q/l^2$, F_Q stands for the source area, l for the length of the flight path between source and target and ν for the pulse frequency. The intensity is therefore invers proportional to the square of the length of the flight path. For experiment with high resolution, the intensity would critically be influenced if neutron guide tubes would not exist. The nickel plated neutron guide tube has according to H. Maier-Leibnitz and T. Springer [25] a critical angle for total reflection given by

$$(8)\quad \gamma = \frac{0.0107}{\varkappa} \quad (\varkappa \text{ in } \text{Å}^{-1})$$

it guarantees therefore a constant collimation for neutron beams leaving a neutron guide tube independent on its length. Apart from a factor for the reflectivity, the intensity at the end of a neutron guide tube is also independent of its length. At a H. F. B. R. of the Grenoble type a bent neutron guide tube conducts thermal and cold neutrons to an area of low background. At a P. P. F. R. the bent neutron guide tube has the same task, but in addition its length is adjusted to the desired resolution, therefore it acts as an effective pulse shortener. The same effect is obtained for thermal, hot and epithermal neutrons by an accelerator driving a P. P. F. R. in booster mode.

It can be shown that for all elastic diffraction experiments and for a number of inelastic scattering experiments using thermal and cold neutrons for the impinging neutron beam the neutron guide tube delivers the desired beam divergence.

For all experiments using neutron guide tubes $d\Omega$ is constant for a given neutron energy and the desired energy-resolution will be adjusted to a given Δt_M by the appropriate length of the neutron guide tube. Consequently all

experiments using neutron guide tubes have maximum intensity if

$$(9) \qquad \bar{\Phi} = \int^{\text{pulse}} \Phi(F.t)\, dt,$$

the time integrated or stationary flux is maximized.

For experiments with geometrical collimation (without guide tube) it follows from equation (6) that $l \approx \Delta t_M = \sigma$ and from (7) that maximum intensity is obtained if

$$(10) \qquad M(\sigma) = \frac{\int^{\text{pulse}} \Phi_1(t)dt}{\sigma^2} \approx \frac{\Phi_1^{\max}[\sigma(d)]}{\sigma(d)}$$

is maximized where σ^2 is given by

$$(11) \qquad \sigma^2 = \int^{\text{pulse}} \Phi_1(t)t^2 dt \Big/ \int^{\text{pulse}} \Phi_1(t)dt$$

and "d" stands for the moderator thickness.

IV. General Considerations for the Basic Design Elements of a Periodically Pulsed Fast Neutron Source

IV. 1. Operational Data and Core Geometry

For a periodically pulsed fast neutron source the average power is constant if

$$(12) \qquad \Phi^f_{\max}(\Delta t^f, \nu).\Delta t^f.\ \nu = \text{constant}$$

At a P. P. F. R. Δt^f is constant and $\Phi^f_{\max}(\Delta t^f, \nu)$ can only be varied with the frequency. At a P. P. F. B. the three parameters can be varied within certain limits.

It is selfevident that the source with the shortest pulse, the lowest frequency and the highest peak flux is the best one. Material strength determines the limiting values. For any fast neutron generator not only a high and constant power is desired, but also a high escape probability for the fast neutrons leaking from the core to the moderators and control elements. Such considerations lead to the "cylindrical-hexagonal" core-geometry as it

has been adopted for SORA and I. B. R. -II. This geometry requires more fuel than a more spherical shape, but it turns out that it is a natural and suitable form for the moderators and bent neutron guide tubes.

IV. 2. The Moderator Geometry and Moderator Composition

From Fig. 9, 10, and 11 follows that the moderators should have a thickness of about 10-12 cm to obtain a maximized stationary flux, which has to be extracted by reentrant channels. Most of the neutron guide tubes will be bent and not straight having a cross section of $\sim 25 \times 3 \sim$ cm^2, very suitable for the design of reentrant channels. Pulsed neutron sources have a relative low mean power, therefore large beam tubes can be designed and large source areas are useful. The projected SORA-moderators have diameters of 28 cm and a height of 36 cm. Fig. 12 shows a cross section of the SORA-core and moderators. Fig. 13, 14 and 15 give details and alternatives to the moderator-configuration of Fig. 12.

The thermal neutron source ought to be H_2O at room temperature if ZrH_2 has not to be used for safety reasons. The axial escape probability should be reduced in any case by plates of ZrH_2 about 1 mm thick, mounted in the reentrant channel at a distance of 5 cm in height.

The cold source consists in any case of two moderator materials: H_2O (ZrH_2) at room temperature and Para-Wasserstoff at 20°K. The water serves as heat shield and slowing down medium, the Para-H_2 as cold neutron source. For the cold source design as projected for SORA and sketched in Fig. 13, the cooling power in the liquid H_2 part would be about 20 Watt.

The hot source consists as well of two moderator materials: a metal hydride at elevated temperatures and BeO at 2000°C. It is not yet clear if ZrH_2 at 850°C, TiH_2 at 600°C or YH_2 at 1200°C should be used. The moderator material will be the best for which the highest population of the first excited level of the Proton-Einstein-Oscillator and the highest proton density will be obtained.

The ultra cold neutron source is sketched in Fig. 16. It has to be located as close as possible to the cold source, in the case of SORA in a slanted beam tube. The pulse duration of ultra cold neutrons will be about 200 μsec. Hydrogen has a negative scattering length, consequently the index of refraction given by

$$(13) \quad n = 1 - \frac{2\pi}{\varkappa^2} N . a_{coh}$$

is larger than unity and therefore the ultra cold neutrons are slowed down by leaving the moderator. A rotating shutter installed in front of a neutron guide tube allows the filling of neutron bottles with a neutron density proportional to the peak flux of the ultra cold neutron source. The low γ - and (n, γ)-heating allows a rather inexpensive design of this source.

IV. 3. The Beam Tube Dimensions

As already mentioned, the bent neutron guide tubes require at least in one dimension large beam channels. In general large neutron source areas are desired and consequently large beam tubes have to be designed. In Fig. 17 neutron scattering experiments with and without neutron guide tubes are sketched in real and in inverse space according to H. Maier-Leibnitz /26/. For intensity reason all neutron scattering experiments should use a 4π -detection geometry which requires a symmetric momentum space element in the direction of the impinging neutron beam. Even bent neutron guide tubes with their rectangular cross section produce symmetric neutron beams in momentum space. For experiments without neutron guide tubes it follows from Fig. 17 that the beam channel should have a cylindrical shape. For all reflections, except the backscattering reflections, a symmetric momentum space element is requested. From that follows:

$$(14) \quad \Delta t_M = \sigma = \frac{d}{v}$$

where "d" stands for the beam tube diameter and v for the neutron velocity. For a beam tube diameter of d = 24 cm and a neutron velocity of v = 3000 m/sec

one obtains

$$(15) \quad \Delta t_M = \sigma = \frac{0.24}{3000} = 80\ \mu\text{sec}$$

a moderator pulse length obtainable from an optimized neutron source of a P. P. F. R. For all neutrons with $v < 3000$ m/sec the momentum space elements are flat, particularly well suited for back-scattering reflections, which amount to about half of all possible reflections.

For the following reasons beam tubes with large diameters can be installed in a P. P. F. R. of some MWatt mean power:

- No neutron flux depression is coupled with large beam tube diameters
- Due to the self-shielding effects of the fast core the γ-heating is rather low and due to the low mean neutron flux (n, γ) and (n, p) processes do not endanger the beam tubes
- All horizontal beam channels are used for white neutron beam experiments; therefore the large beam tubes can be shielded easily. The target stations are all outside the reactor hall. The concrete shield extends up to the reactor hall and outside the reactor hall the beam tubes and neutron guide tubes are embedded in water basins, see Fig. 18.
- The horizontal beam tubes in the reactor block have increasing diameter from the inner to the outer side to allow the installation of manifolded funnel-like neutron guide tubes, which allow at a certain distance from the core the connection of 5 separate neutron guide tubes, see Fig. 19. Due to the low γ-heating and fast neutron flux, the installation of such manifolded funnel-like neutron guide tubes is possible at a close distance from the source.
- All slanted beam tubes are used for monochromatic neutrons with collimation in the reactor block already, they do not pose a shielding problem, see Fig. 18.

IV. 4. Operation-Frequency

All neutrons leaking from the moderators into the beam channels ought to be used possibly for experiments. Therefore all horizontal beam tubes are used for white neutron beam experiments. From Fig. 20 it follows that for a given operation frequency and a given length l of the flight path an overlap of neutrons from successive neutron source pulses can only be avoided if

$$(16) \quad \frac{v_{max} - v_{min}}{v_{max} \cdot v_{min}} \cdot l = \frac{\Delta v}{\bar{v}} \cdot \frac{l}{\bar{v}} = T = \frac{1}{\nu}$$

For $\nu = 50$ cycles/sec, $v = 500$ m/sec and $l = 100$ m one obtains for $\Delta v/\bar{v} = 0.1$. Only a very small fraction of all neutrons can be accepted in this high resolution experiment. So-called overlap-rotors must limit the acceptable velocity band width as indicated in Fig. 20. For an operation frequency of $\nu = 5$ cycles/sec the useful velocity band width can be increased by a factor of 10 which corresponds to a true intensity gain since these neutrons are not absorbed any more in the overlap-rotors. Hence the lowest possible operation frequency is always the best, it is determined by the maximum acceptable temperature jump in the fuel element, the associated stress in the canning material and in general on the thermo-mechanical properties of the reactor core. The lowest possible operation frequency of a periodically pulsed neutron source can only be approached after a certain operation experience and an extended fuel test program.

IV. 5. Background Problems

In the case of SORA with $\nu = 50$ cycles/sec the ratio of maximum power to power between pulses is

$$(17) \quad \frac{P_{max}}{P_{min}} \approx 1200$$

and the corresponding value for thermal neutrons

$$(18)\quad \frac{\Phi^{th}_{max}}{\Phi^{th}_{min}} \approx 700$$

For a white neutron beam experiment without overlap-rotors, neglecting effects of fast neutrons (bent neutron guide tube), the signal to background ratio is

$$(19)\quad \frac{\text{signal}}{\text{background}} = \frac{\Phi^{th}_{max}}{\Phi^{th}_{min}} \cdot \frac{\Delta t_M}{T} = 700 \cdot \frac{10^{-4}}{20.10^{-3}} = 3.5$$

Even with the reduction of $\nu = 1/T$ by a factor of 10, the result is not satisfactory. The use of overlap-rotors is unavoidable even for bent neutron guide tubes. From Fig. 20 follows that the useful velocity band width is coupled to the duration of the background pulse length. The first overlap-rotor should be as close to the neutron source as possible.
One obtains:

$$(20)\quad \frac{\text{signal}}{\text{background}} = \frac{\Phi^{th}_{max}}{\Phi^{th}_{min}} \cdot \frac{\Delta t_{moderator}}{\Delta t_{overlap\text{-}rotor}} \quad \frac{700}{1} \cdot \frac{10^{-4}}{2.10^{-3}} = 35$$

As I will show in the second lecture, this background problem can be solved with a statistical chopper in the "quasi-monochromatic" beam at the end of a neutron guide tube; on the expense of 50% of the intensity a $S/B \approx 10^{+3} - 10^{4}$ ought to be obtained. For a number of diffraction experiments such S/B values are requested.

IV.6. The Pulse Shape Problem

Fig. 21 and 22 show the results of time dependent Monte Carlo calculations by H. Rief /22/ for two H_2O moderators with and without reentrant hole. It is obvious that for the cold and hot neutrons one obtains rather symmetric pulse shapes, while for neutrons in the energy range between 10 and 200 MeV the pulses show a slight asymmetry for the SORA pulsed reactor. In Booster mode the asymmetry will be rather pronounced and as Prof. Dr. L. Dobrzynski /27/ showed, severe draw-backs for a certain number of

experiments are the consequence. If the SORA-moderators are slightly poisoned, one can obtain rather symmetric pulses at all neutron energies. For SORA in booster-mode the moderators will have to be poisoned very strongly in order to obtain a symmetric resolution function. For all experiments without neutron guide tubes, where $M_G(\sigma)$ determines the intensity of an experiment, this is no draw-back at all, but for all experiments with neutron guide tubes, where $\bar{\Phi}$ is the interesting parameter, the loss in intensity is proportional to the reduction of the pulse width.

One can conclude again that for experiments in the range of neutron guide tubes the benefits of the P. P. F. B. compared to the P. P. F. R. are marginal. The benefits of the P. P. F. B. appear for all inelastic and inelastic magnetic scattering energies for neutrons above thermal energies.

V. The Design Elements of the SORA-Reactor for Physics Experiments

V. 1. The Characteristic Design Data of the SORA Reactor

SORA has a compact liquid metal cooled score. The power is pulsed by means of rapid reactivity changes, which are produced by a fast moving reflector block. About half of the fast neutrons produced in the core leak into the reflector, where the reactor controls and the experimental neutron sources are located. The neutron sources are specially designed moderators, which shift the neutron energies into the ranges required by the experiments: $0 \leq E_n \lesssim 1$ MeV. From these neutron sources the "tailored neutron beams" are leaking into the experimental channels of the reactor. The characteristic performance data of the SORA reactor are summarized in Tab. 3.

Table 3 - Principal Reactor Operating Characteristics

Average Power	: $\bar{P}$ = 1 MWatt
Peak Power	: P_{max} = 225 MWatt
Pulse Frequency	: ν = 50 sec^{-1}

Table 3 (contd.)

Power Pulse Half Width	: $\Delta\Theta = 65 \times 10^{-6}$ sec
Thermal neutron peak flux	: $\Phi = 1.5 \times 10^{-15}$ n/cm^{2}sec
Thermal neutron pulse width	: $\Delta t = 120 \times 10^{-6}$ sec
Epithermal neutron peak flux in the energy group 0.43 - 1 eV	: $\Phi_{max}^{epi} = 1.6 \times 10^{14}$ n/cm^2 sec eV
Fast neutron peak flux at core surface	: $\Phi_{max} = 7.5 \times 10^{15}$ n/cm^2 sec
Time average fast neutron flux at core surface	: $\bar{\Phi}_f = 3 \times 10^{13}$ n/cm^2 sec

Fig. 23 shows a horizontal and Fig. 24 a vertical cross section of the reactor. The beam channels labeled with "H" and "S" indicate the position of "Horizontal and 40° upwards "Slanted" beam tubes.

The reactor has:

- 2 epithermal neutron beam channels C 1 H and C 2 H with a total opening collimation of 10° allowing the installation of a large number of simultaneous experiments with a flight path length up to 900 meters,
- 7 beam tubes viewing the cold neutron source: C 3 H, C 3 S, C 4 H, C 4 S, C 5 H, C 6 SL and C 7 H,
- 4 beam tubes viewing the thermal neutron source: C 8 H, C 8 S, C 9 H and C 9 S,
- 7 beam tubes viewing the hot neutron source: C 10 H, C 10 S, C 11 H, C 11 S, C 14 H, C 14 S, C 15 HL,
- 1 tangential beam tube crossing the cold neutron moderator: C 13 T,
- 1 slanted irradiation tube C 12 J viewing the core vessel surface above the hot neutron moderator,
- 1 special beam tube C 11 HS for diffraction experiments with samples under extreme pulsed conditions,
- 10 neutron guide tubes at channel C 4 H and C 8 H, each with a length between 50 and 200 meters. (As it can be seen from Fig. 25, any horizontal beam tube - if required - can be equipped with neutron guide tubes with a length between 100 and 300 meters).

The horizontal beam tubes C 3 H till C 15HL are viewing a source area of 14 x 28 cm^2 while C 1 H and C 2 H have a diameter of 35 cm close to the epithermal neutron souce. The slanted ones have a tube diameter of 14 cm close to the neutron sources except one, the C 6 SL, which has a diameter of 25 cm to accomodate an ultra-cold neutron source. Fig. 25 shows the availability of a suitable site for the SORA-Reactor in the J.R.C. at Ispra. The site is flat, a suitable place to locate a pulsed reactor with its beam tubes.

V.2. The Development Potential of the SORA-Reactor

For practical reasons an operation frequency of ν = 50 cycles/sec and an average power of 1 MWatt has been adopted for the SORA-startup phase. After a certain operation experience and with a detailed knowledge on the fuel behaviour under pulsed operation conditions, the operation frequency will be lowered stepwise to ν = 5 cycles/sec. At the same time the average power could be raised to 3 MWatt. A reduction of the pulse frequency ν in favour of higher peak flux improves:

1. The signal to background ratio,
2. The reaction rate for experiments depending on ϕ^2,
3. The monoenergetic neutron beam experiments applying high pressure or high magnetic and electrical fields on the sample for the investigation of transient states,
4. The neutron economy at the quasi-white neutron beam experiments for higher order diffraction and incoherent inelastic scattering experiments,
5. Transient phenomena and transport mechanism,
6. The accuracy of neutron decay measurements using neutron bottles.

Provisions have been made to install at a later time a linear electron accelerator of 200 kWatt beam power.

VI. Literature

1) HENDRIE, J.M. and KOUTS, H.J.C.
Proceedings of a Seminar on "Intense Neutron Sources", Santa Fe, New Mexico, 19-23 September 1966
CONF-660925, U.S.A.E.C. and E.N.E.A.

2) BECKURTS, K.H., DAUTRAY, R.
Proceedings of a Seminar on "Intense Neutron Sources", Santa Fe, New Mexico, 19-23 September 1966
CONF-660925, U.S.A.E.C. and E.N.E.A.

3) COLE, T.E.
Proceedings of a Seminar on "Intense Neutron Sources", Santa Fe, New Mexico, 19-23 September 1966
CONF-660925, U.S.A.E.C. and E.N.E.A.

4) DE HOFFMANN, F., FELD, B.T. and STEIN, P.R.
Delayed Neutrons from U-235 after short irradiation
Phys. Rev., 74, p. 1330 (1948)

5) PAXTON, H.C.
Critical Assemblies at Los Alamos
Nucleonics, 13, No. 10, p. 48 (1955)

6) WIMETT, T.F. and ORNDOFF, J.D.
Application of Godiva II Neutron Pulses
1958 Geneva A/CONF. PUAE 10, p. 449 (1958)

7) WIMETT, T.F. et al.
Godiva II, an Unmoderated Pulse-Irradiation Reactor
Nucl. Sci. and Eng., 8, p. 691-708 (1960)

8) BONDARENKO, I.I., STAVISKII, Yu. Ya.,
Atomnaja Energija 7, 417 (1959), Reactor Sci. Technology (J.N.E. Part A/B) 14, 55, (1961)

9) BLOKHIN, G.E. et al.
Atomnaja Energija 10, 437 (1961)

10) BUNIN, B.N. et al.
Proceedings 3rd U.N. Int. Conf. PUAE 7, 473, (1964)

11) RAIEVSKI, V., KLEY, W., ASAOKA, T., BLAESSER, G., CALIGIURI, G.P., HAAS, R., KISTNER, G., KSCHWENDT, H., LARRIMORE, J.A., MATTHES, W., MISENTA, R., MØLLER, H.B., QUIQUEMELLE, B., RICCOBONO, G., RIEF, H., WUNDT , H.,
EUR-1643 e, p. 51-81 (1964)

12) RAIEVSKI, V., KLEY, W., HAAS, R., LARRIMORE, J., ASAOKA, T., GIEGERICH, K., MISENTA, R., RANDLES, J., RICCOBONO, G., RIEF, H., SCIUTO, F., WUNDT , H., TAVERNIER, G., VAN DIEVOT, J.,

VAN MIEGROET, J., HILDENBRAND, H., SCHWARZ, H.R.
The Pulsed Fast Reactor as a Source for Pulsed Neutron Experiments, Proc. I.A.E.A., Symp. Pulsed Neutron Research, Karlsruhe, May 1965, Vol. II, p. 553-573

13) HAAS, R., MØLLER, H.B.,
EUR-490 e, (1963)

14) KLEY, W.,
EUR-2538 e, (1965)

15) KLEY, W.,
I.A.E.A.-Panel on Kinetics and Applications of Pulsed Research Reactors, Vienna, May 17-21, (1965)

16) KLEY, W.,
I.A.E.A.-Panel on Research Applications of Nuclear Pulsed Systems, Dubna, July 18-22, (1966)

17) KLEY, W.,
Proc. Intern. Conference on Research Reactor Utilization and Reactor Mathematics, Mexico City, May 1967, EUR-4082 e, (1968)

18) LARRIMORE, J.A., HAAS, R., GIEGERICH, K., RAIEVSKI, V., and KLEY, W.,
AEC-ENEA-Seminar on Intense Neutron Sources, Santa Fe, U.S.A., September (1966)

19) Proceedings of the Joint Euratom-Japanese Information Meeting on the Design Status and the Projected Use in Science and Technology of the Euratom Project SORA and the Japanese Lineac Booster Project, held at Ispra, September 17-18, (1971)
EUR-4954-e, (1971)

20) ANANEV, V.D., BLOKHINTSEV, D.I., BUNIN, B.N., FRANK, I.M., KULKIN, L.K., MATORA, I.M., NAZAROV, V.M., RUDENKO, V.T., SHABALIN, E.P., SHAPIRO, F.L., and YASVITSKII, Yu. S.,
Proc. of the National Topical Meeting on Fast Burst Reactors held at the University of New Mexico, Albuquerque, Jan. 28-30, (1969)

21) ANANʹEVETAL, V.D.,
Proceedings of the Fourth International Conference, Geneva, 6-16 September (1971), Vol. 7, p. 41-52

22) ASAOKA, T., RIEF, H.
Proceedings of the Joint Euratom-Japanese Information Meeting on the Design Status and the Projected Use in Science and Technology of the Euratom Project SORA and the Japanese Lineac Booster Project, held at Ispra on Sept. 17-18, (1971),
EUR-4954-e (1971)

23) KLEY, W.
Proceedings of the Joint Euratom-Japanese Information Meeting on the Design Status and the Projected Use in Science and Technology of

of the Euratom Project SORA and the Japanese Lineac Booster Project, held at Ispra on Sept. 17-18, (1971)
EUR-4954 e (1971)

24) RICCOBONO, G., ARDENTE, V., and ROSSI, G.
Proceedings of the Joint Euratom-Japanese Information Meeting on the Design Status and the Projected Use in Science and Technology of the Euratom Project SORA and the Japanese Lineac Booster Project, held at Ispra on Sept. 17-18 (1971)
EUR- 4954 e (1971)

25) MAIER-LEIBNITZ, H., SPRINGER, T.
Reactor Sci. and Technology, 17, 217 (1963)

26) MAIER-LEIBNITZ, H.
Nukleonik, 8, 61 (1966)

27) DOYLE, T. A.
Proceedings of the Joint Euratom-Japanese Information Meeting on the Design Status and the Projected Use in Science and Technology of the Euratom Project SORA and the Japanese Lineac Booster Project, held at Ispra on Sept. 17-18 (1971)
EUR-4954 e (1971)

VII. Figure Captions

Fig. 1 Beam Tube Distribution of the H. F. B. R. Grenoble

Fig. 2 The Theoretical Differential Flux Distribution in the Different Neutron Sources of the H. F. B. R. Grenoble (Solid Lines) and of the SORA-Hot-Source (Dashed line, ZrH_2 at T = 700°K, Reentrant Hole, P = 1 MW, ν = 50 cycles/sec).

Fig. 3 The Theoretical Differential Flux Distribution in the Different Neutron Sources of the H. F. B. R. -Grenoble (Solid Lines) and of the SORA-Thermal Source (Dashed Line, H_2O at T = 300°K, Reentrant Hole).

Fig. 4 The Theoretical Differential Flux Distribution in the Different Neutron Sources of the H. F. B. R. -Grenoble (Solid Lines) and of the SORA-Cold Source (Dashed Line, H_2O at T = 300°K and Para-H_2 at T = 20°K, Reentrant Hole)

Fig. 5 Schematic Drawing of the I. B. R. -I

Fig. 6 Gain-Factor $M_G(E)$ for the Cold Neutron Source

Fig. 7 Gain-Factor $M_G(E)$ for the Thermal

Fig. 8 Gain-Factor $M_G(E)$ for the Hot Neutron Source

Fig. 9 The Stationary Epithermal Neutron Flux in a H_2O-Slab-Moderator

Fig. 10 The Stationary Thermal Neutron Flux in the Energy Interval; 0.15-0 eV, at the Surface and in the Center of Water Slabs of Various Thicknesses at 300°K

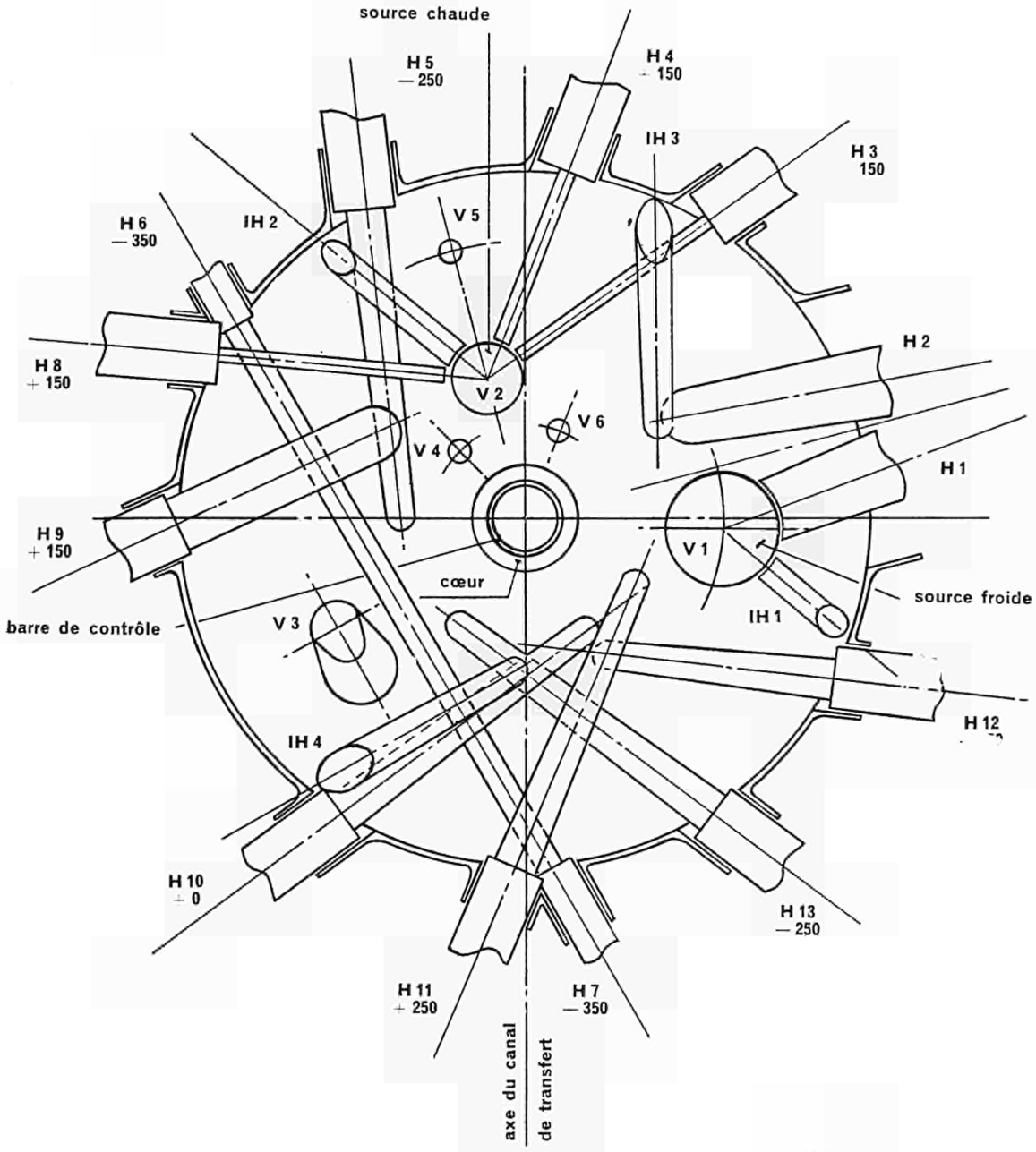

FIGURE 1

RHF / DISPOSITION DES CANAUX DANS LE RÉFLECTEUR

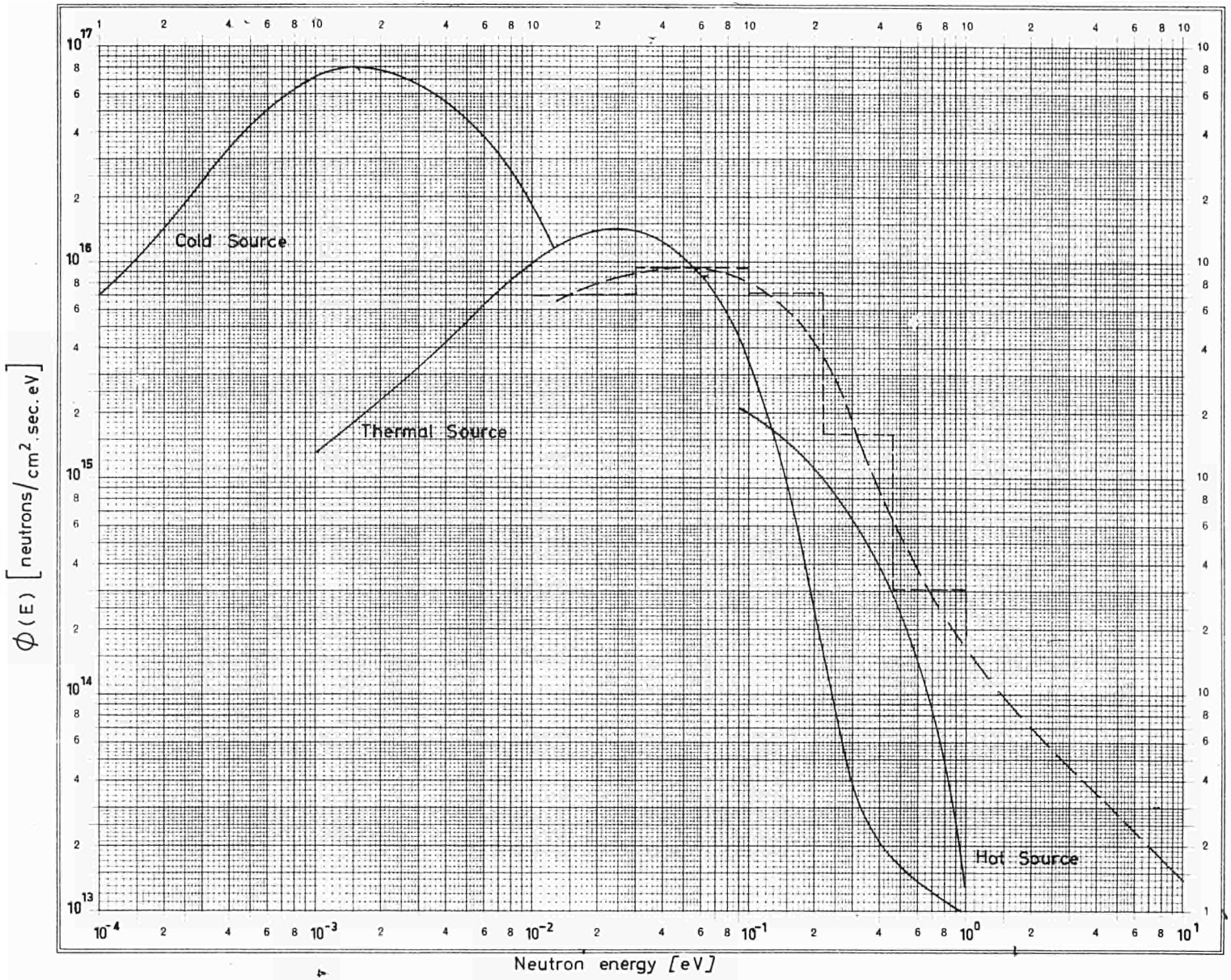

Fig. 2 THE THEORETICAL DIFFERENTIAL FLUX DISTRIBUTION IN THE DIFFERENT NEUTRON SOURCES OF THE H.F.R. - GRENOBLE (SOLID-LINES) OF THE SORA - HOT - SOURCE (DASHED LINE, ZrH_2 AT 700°K, REENTRANT HOLE, $\overline{P}$ = 1 MW, ν = 50 p.p.s.).

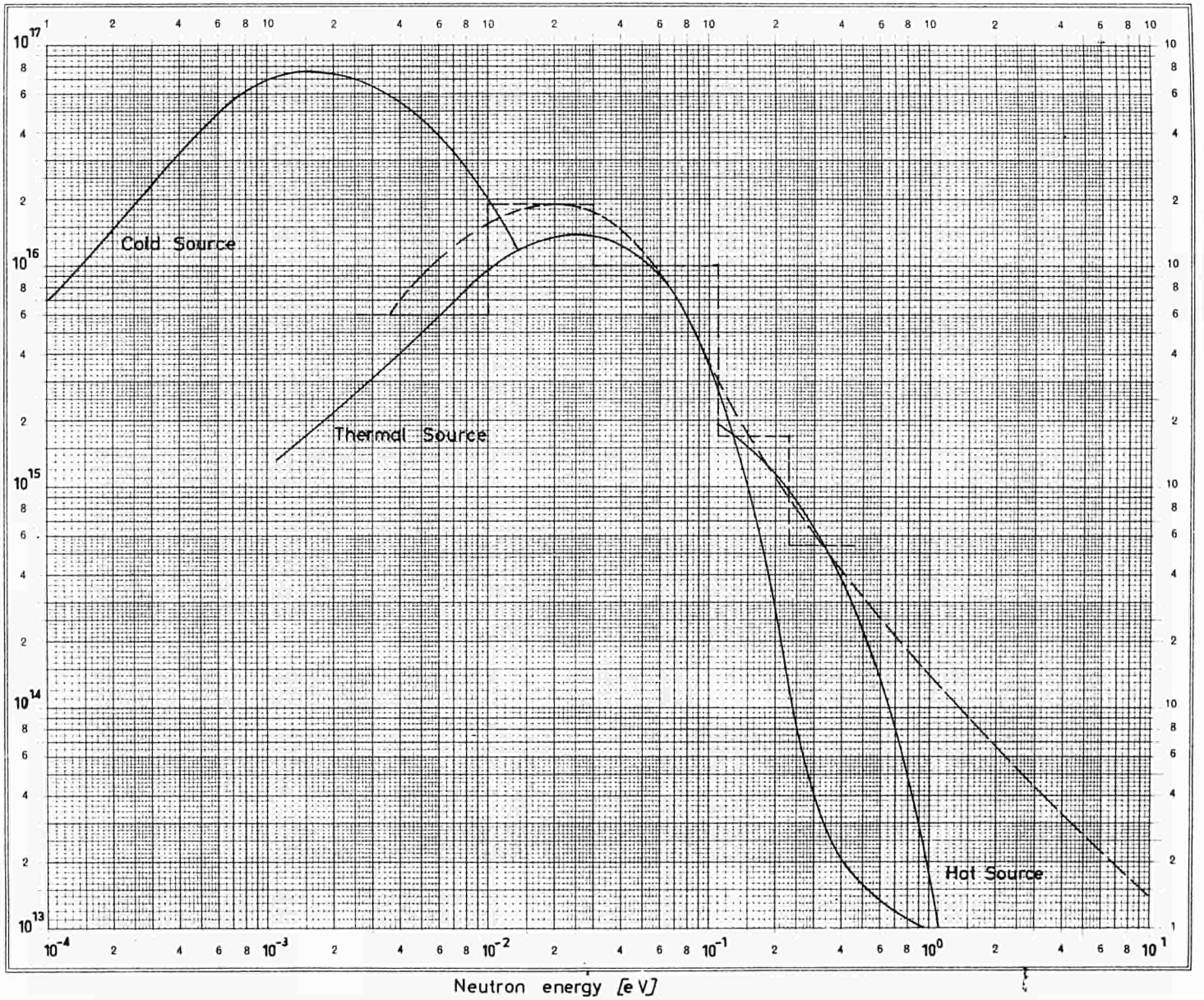

Fig. 3. THE THEORETICAL DIFFERENTIAL FLUX DISTRIBUTION IN THE DIFFERENT NEUTRON SOURCES OF THE H.F.R. - GRENOBLE (SOLID LINES) AND OF THE SORA - THERMAL SOURCE (DASHED LINE, H_2O AT 300° K, REENTRANT HOLE)

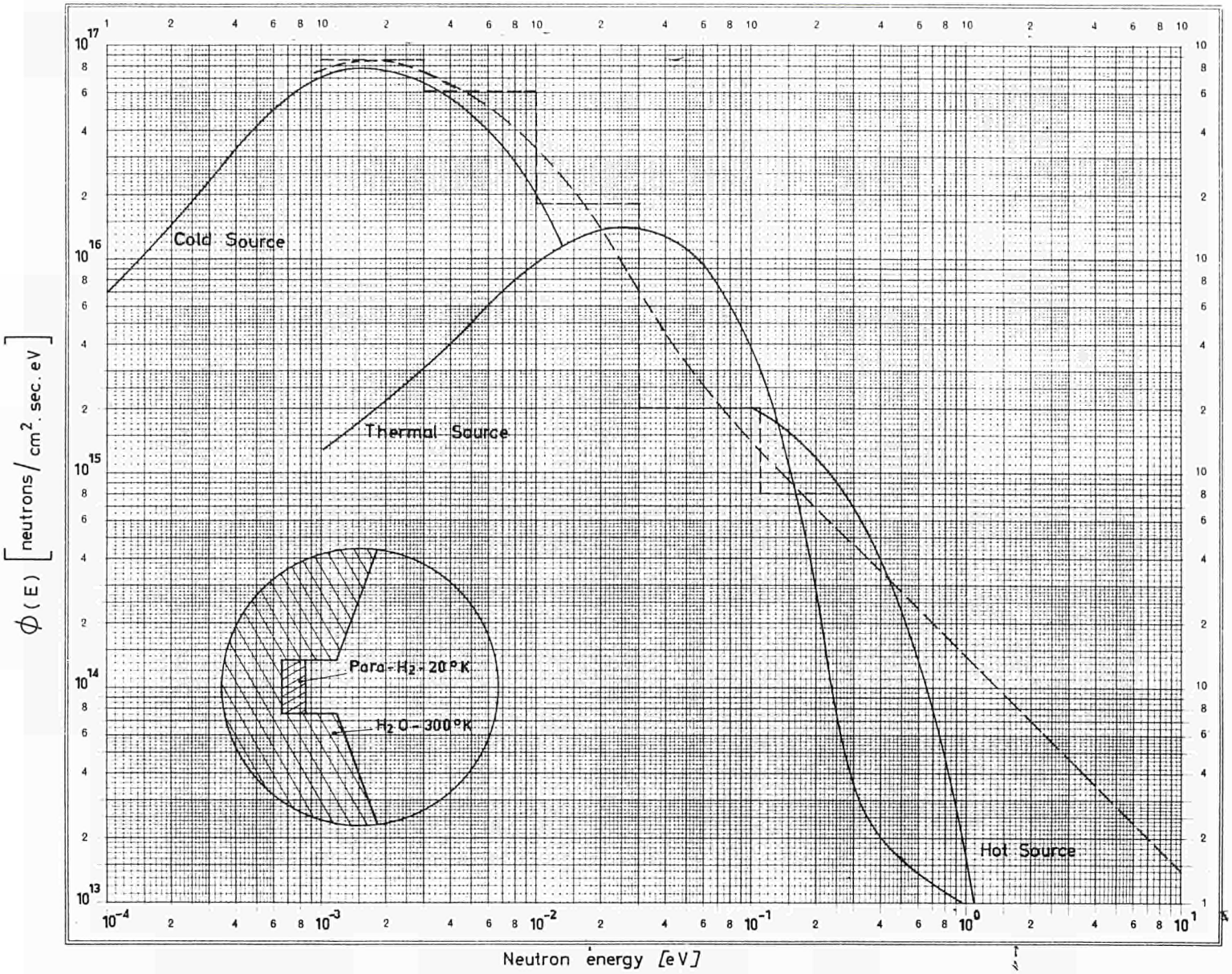

Fig. 4. THE THEORETICAL DIFFERENTIAL FLUX DISTRIBUTION IN THE DIFFERENT NEUTRON SOURCES OF THE H.F.R.- GRENOBLE (SOLID LINES) AND OF THE SORA - COLD - SOURCE (DASHED LINE, H_2O AT 300 °K AND PARA-H_2 AT 20°K, REENTRANT HOLE).

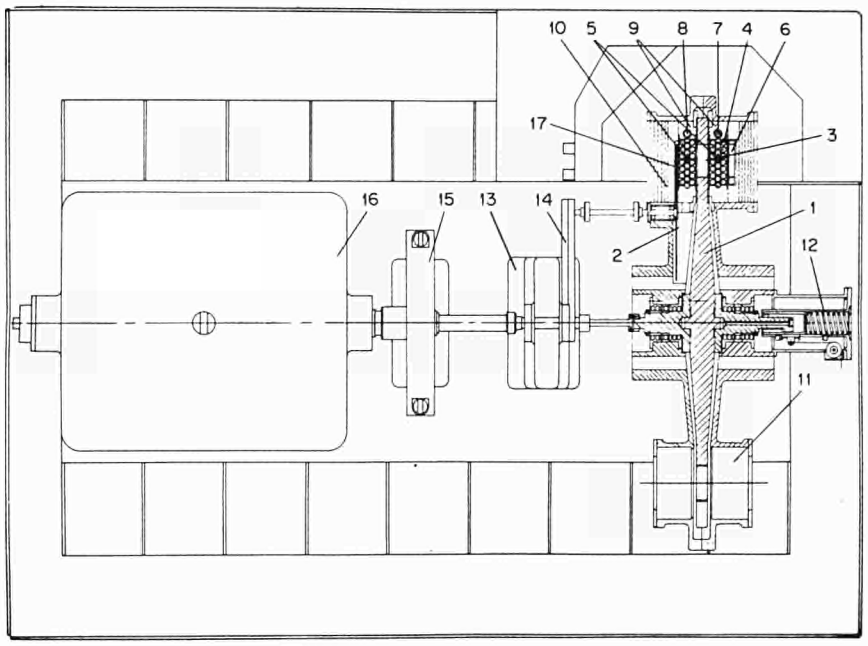

Fig. 5 – Schematic drawing of the IBR. [20]

(1) Rotating disk
(2) Subsidiary disk
(3) Main bushing
(4) Plutonium rods
(5) Scram rods
(6) Coarse control
(7) Automatic regulator rod
(8) Manual control rod
(9) Side reflector
(10) End reflector
(11) Shielding glass
(12) Mechanism for adjustment of main bushing in shielding
(13) Accelerator
(14) Reducing gear of the auxiliary bushing
(15) Brake
(16) Electrical drive
(17) Auxiltary bushing

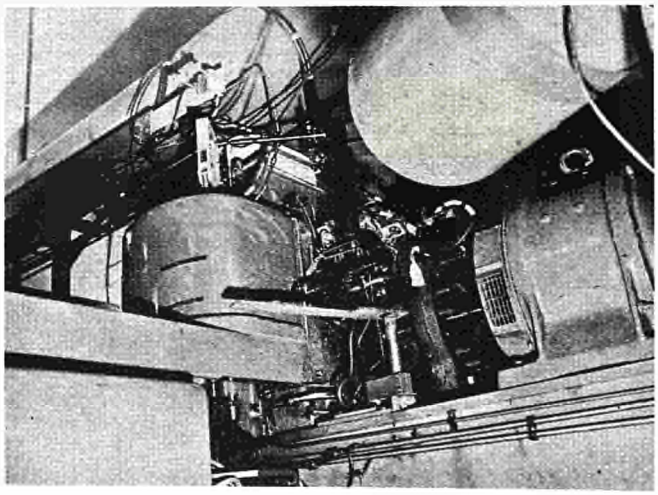

Fig. 5 – General view of the IBR reactor.

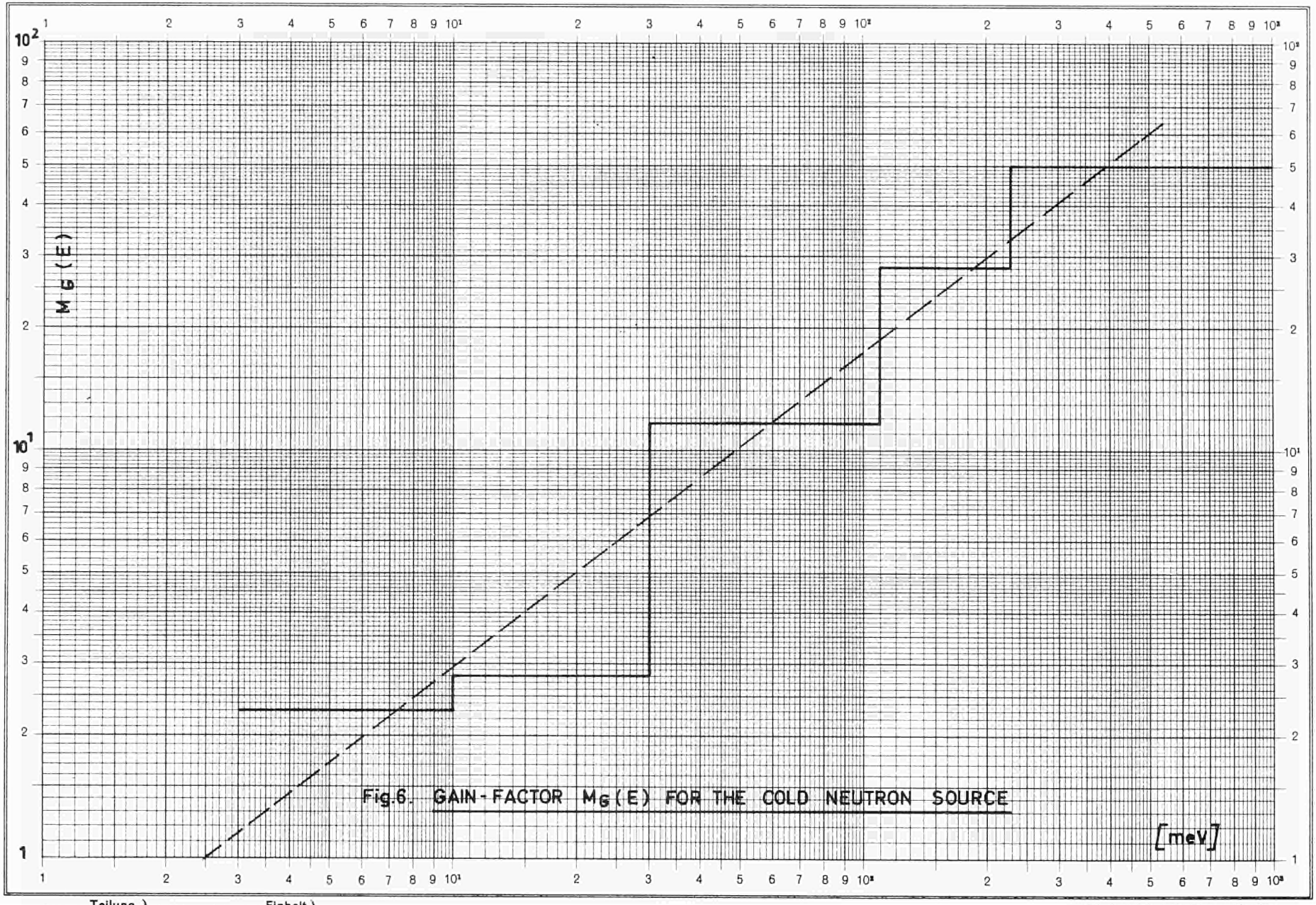

Fig.6. GAIN-FACTOR $M_G(E)$ FOR THE COLD NEUTRON SOURCE

Logar. Teilung / Division } 1-100 und 1-1000 Einheit / Unité } 90 mm

Ed. Aerni-Leuch, Bern Nr. 553

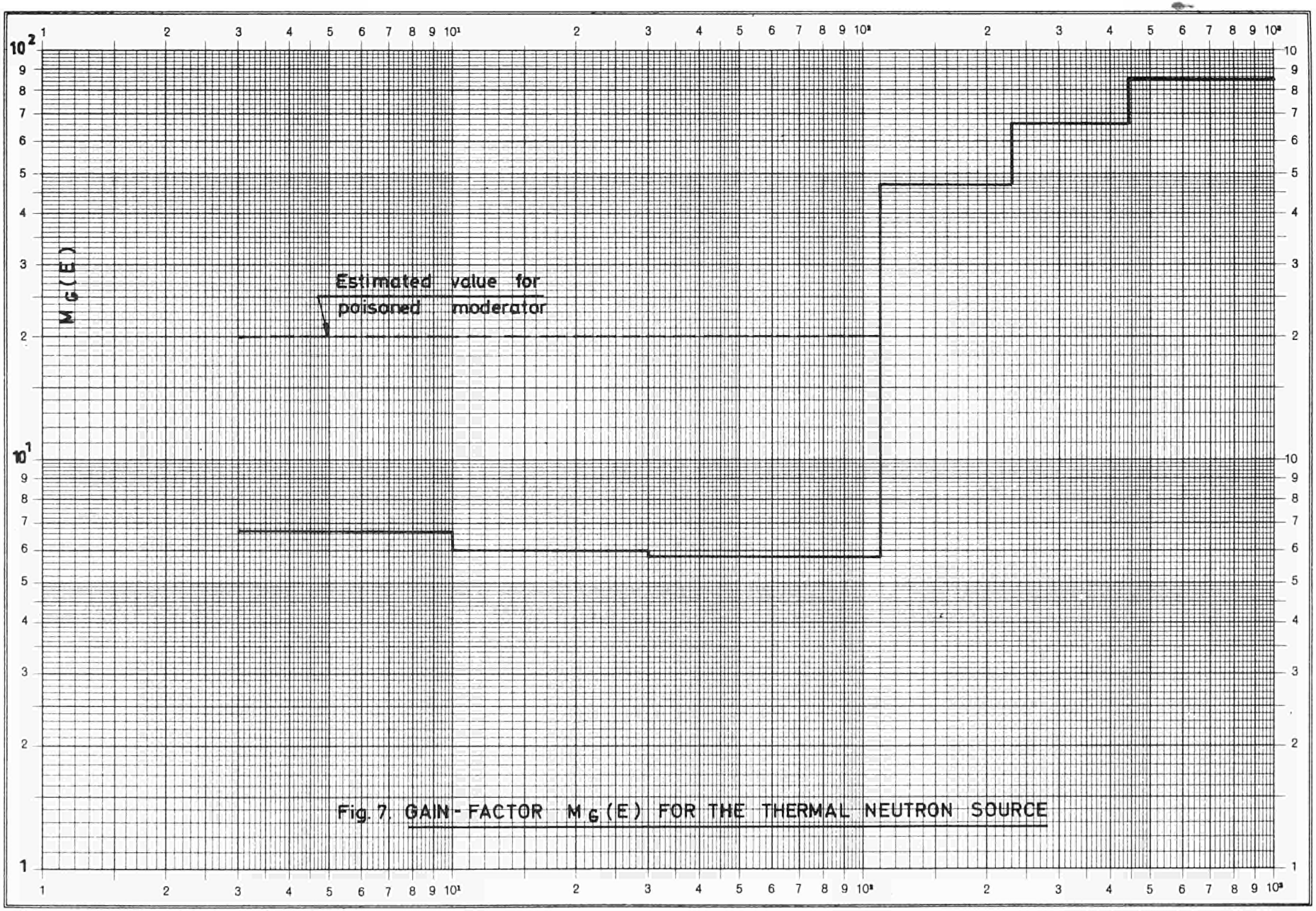

Fig. 7. GAIN-FACTOR $M_G(E)$ FOR THE THERMAL NEUTRON SOURCE

Logar. Teilung / Division } 1-100 und 1-1000 Einheit / Unité } 90 mm

Ed. Aerni-Leuch, Bern Nr. 553

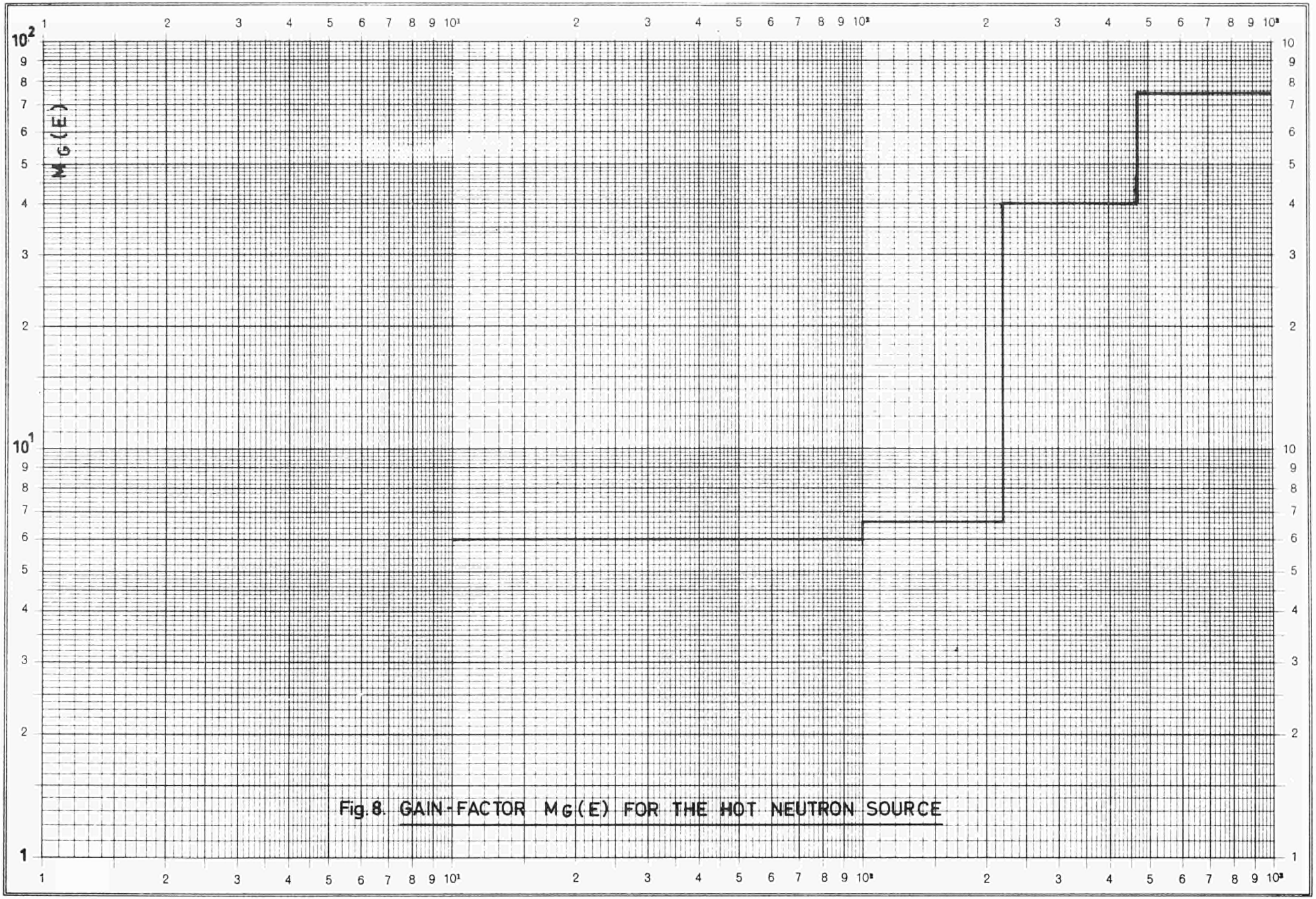

Fig. 8. GAIN-FACTOR $M_G(E)$ FOR THE HOT NEUTRON SOURCE

Logar. Teilung / Division } 1-100 und 1-1000 Einheit / Unité } 90 mm

Ed. Aerni-Leuch, Bern Nr. 553

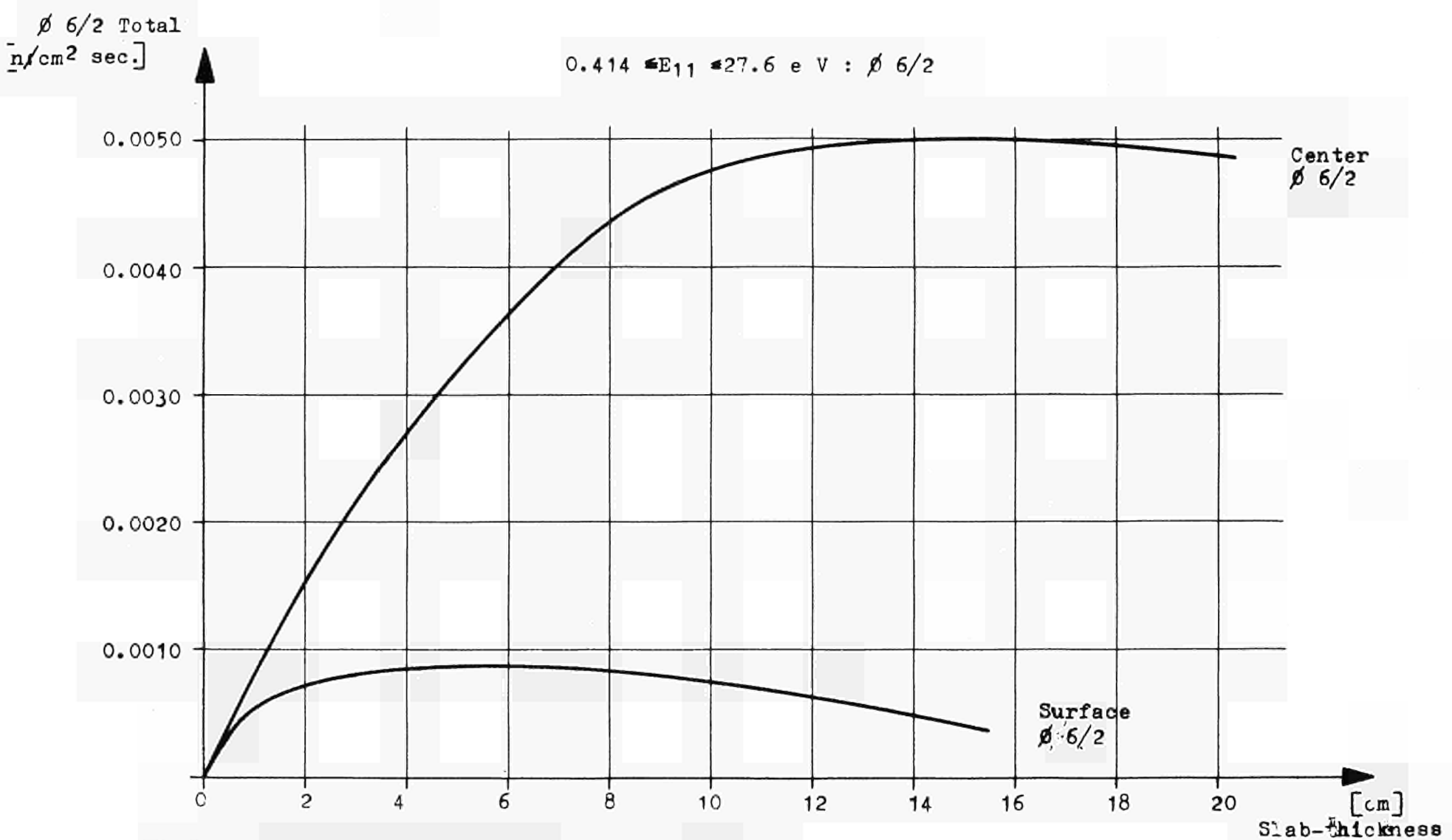

Fig. 9. Epi-thermal neutron flux in a H_2O slab

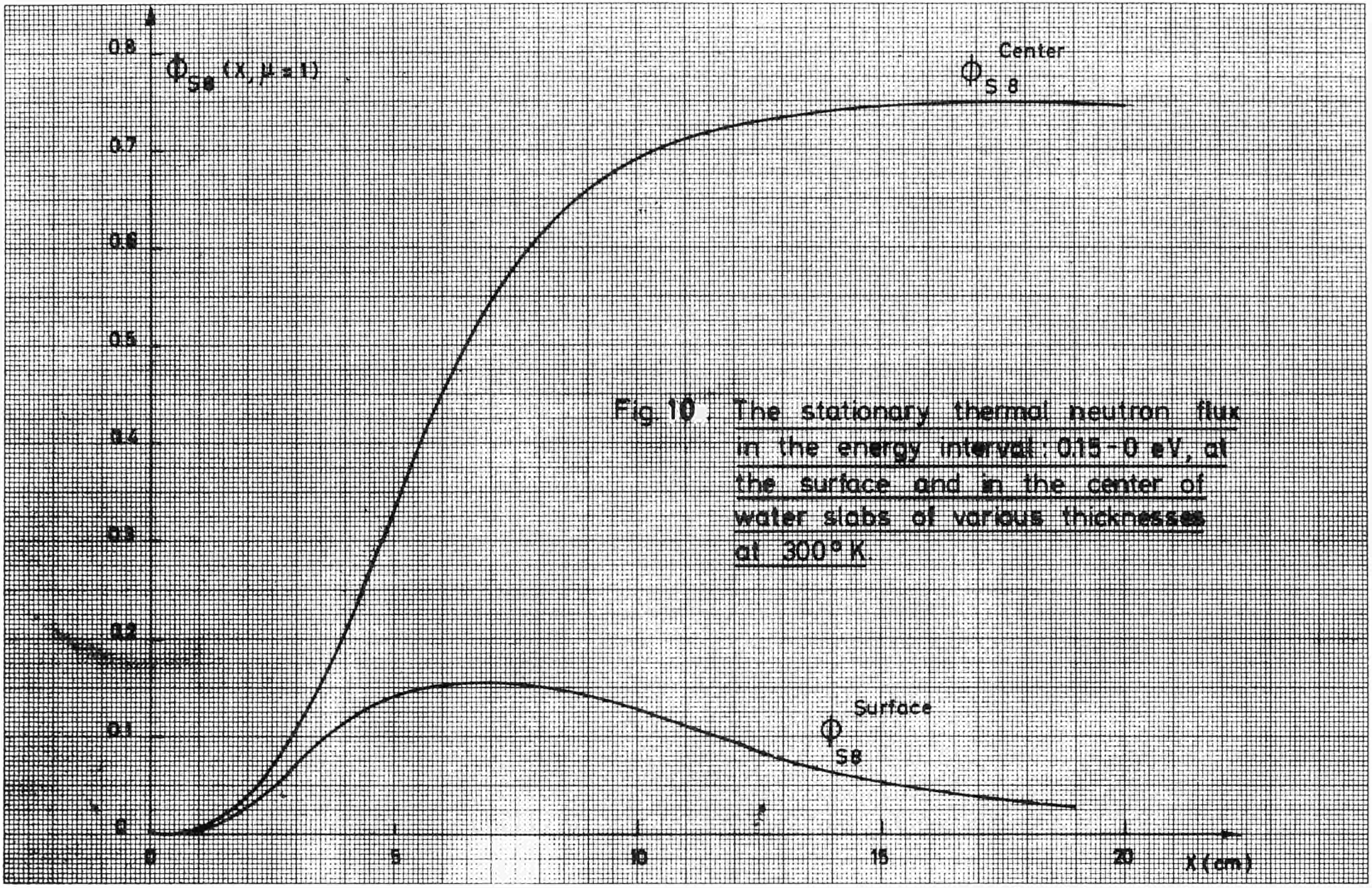

Fig. 10. The stationary thermal neutron flux in the energy interval: 0.15 - 0 eV, at the surface and in the center of water slabs of various thicknesses at 300° K.

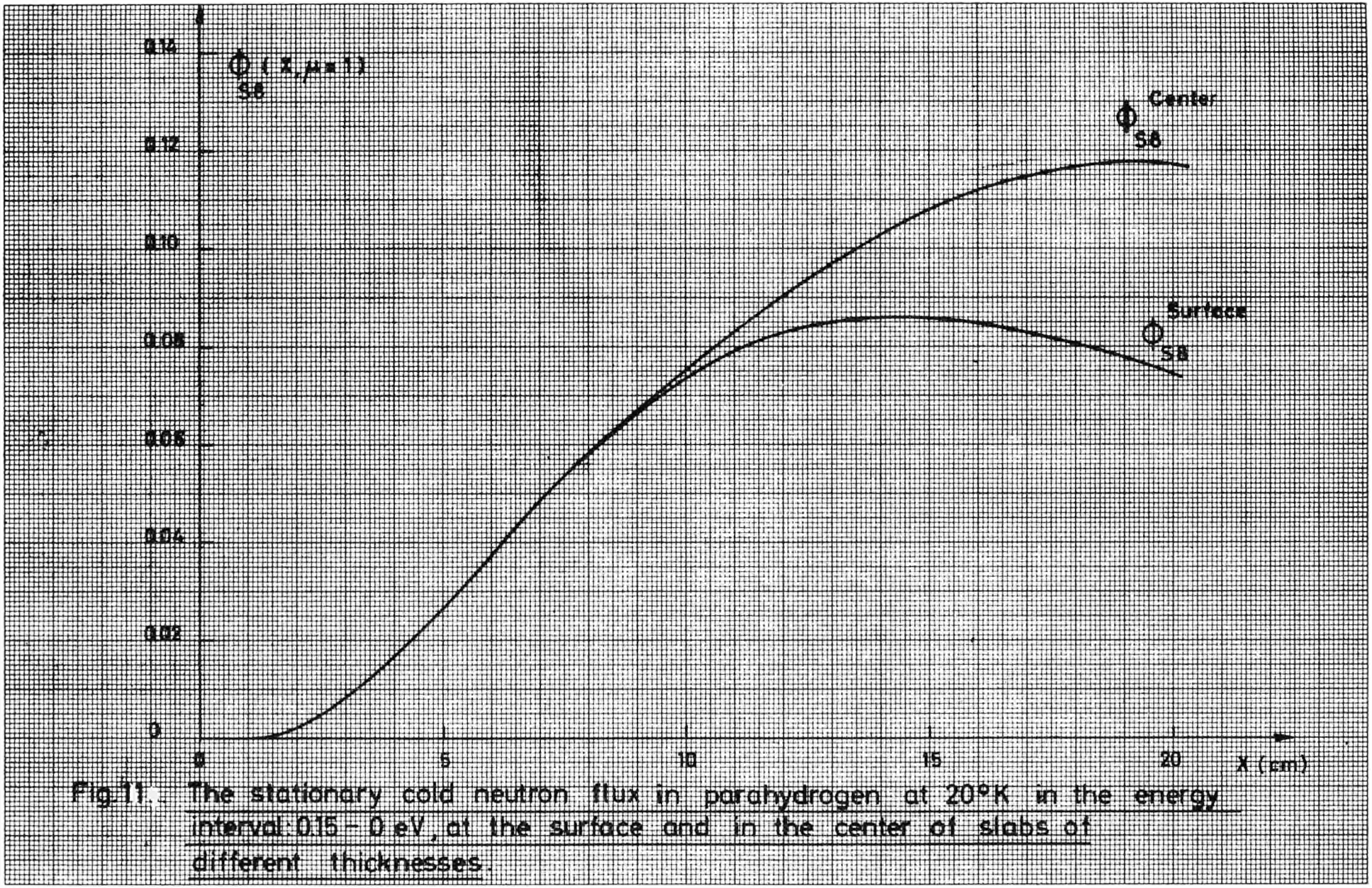

Fig.11. The stationary cold neutron flux in parahydrogen at 20°K in the energy interval 0.15 - 0 eV, at the surface and in the center of slabs of different thicknesses.

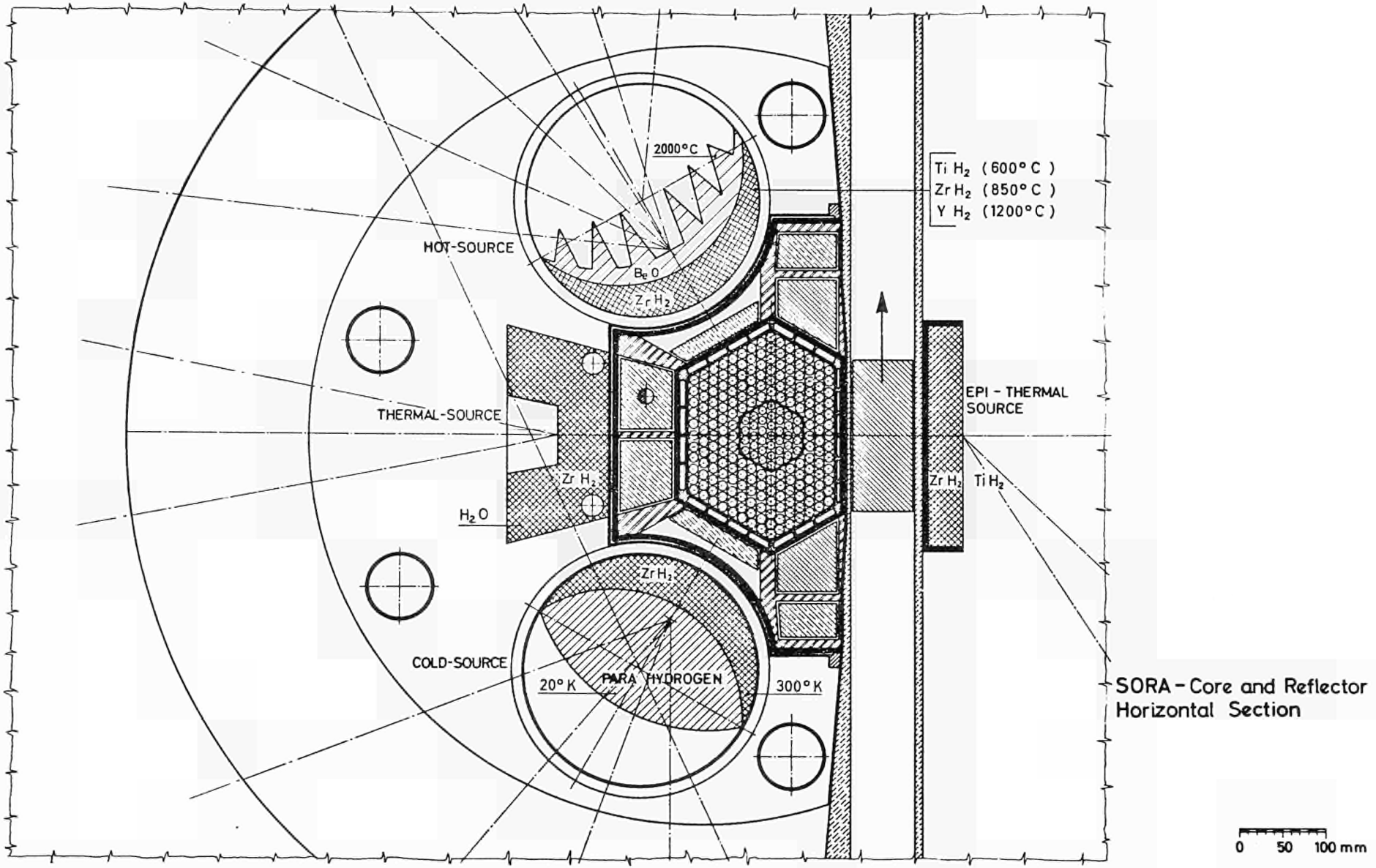

Fig. 12. THE CONCEPTIONAL DESIGN OF THE SORA NEUTRON SOURCES

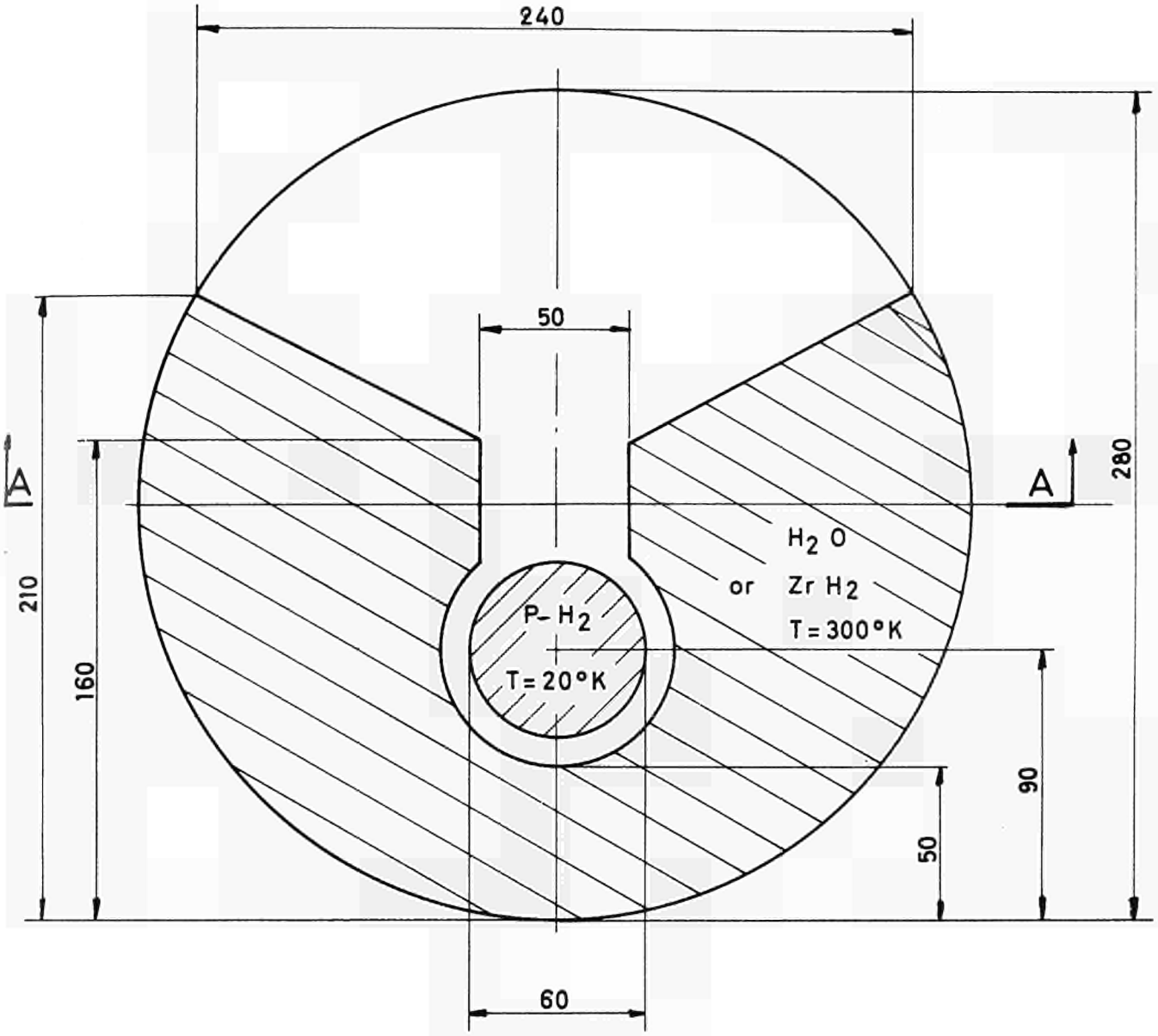

Fig. 13a. Conceptional design of the Cold Neutron Source

Section A-A

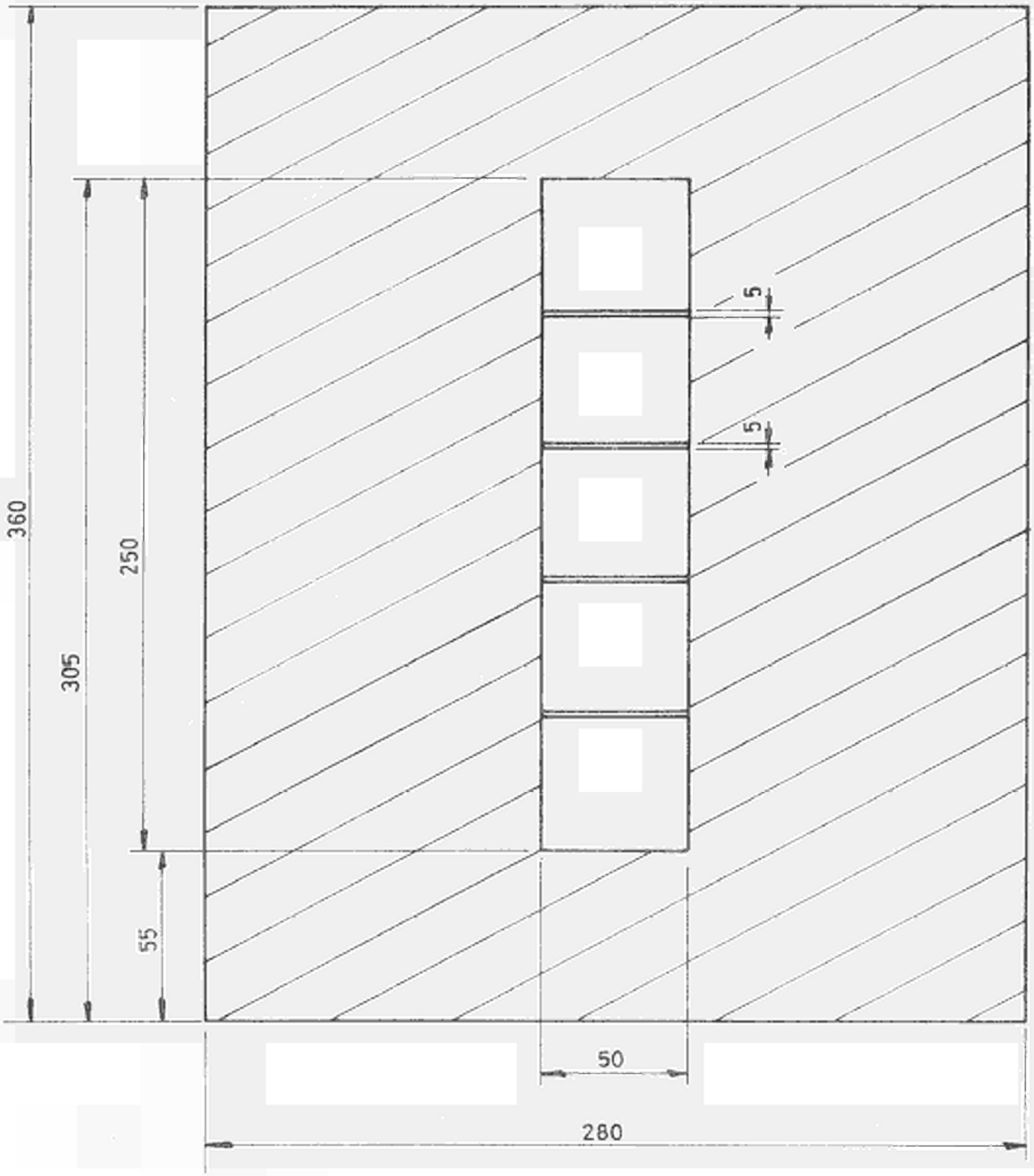

Fig. 13 b

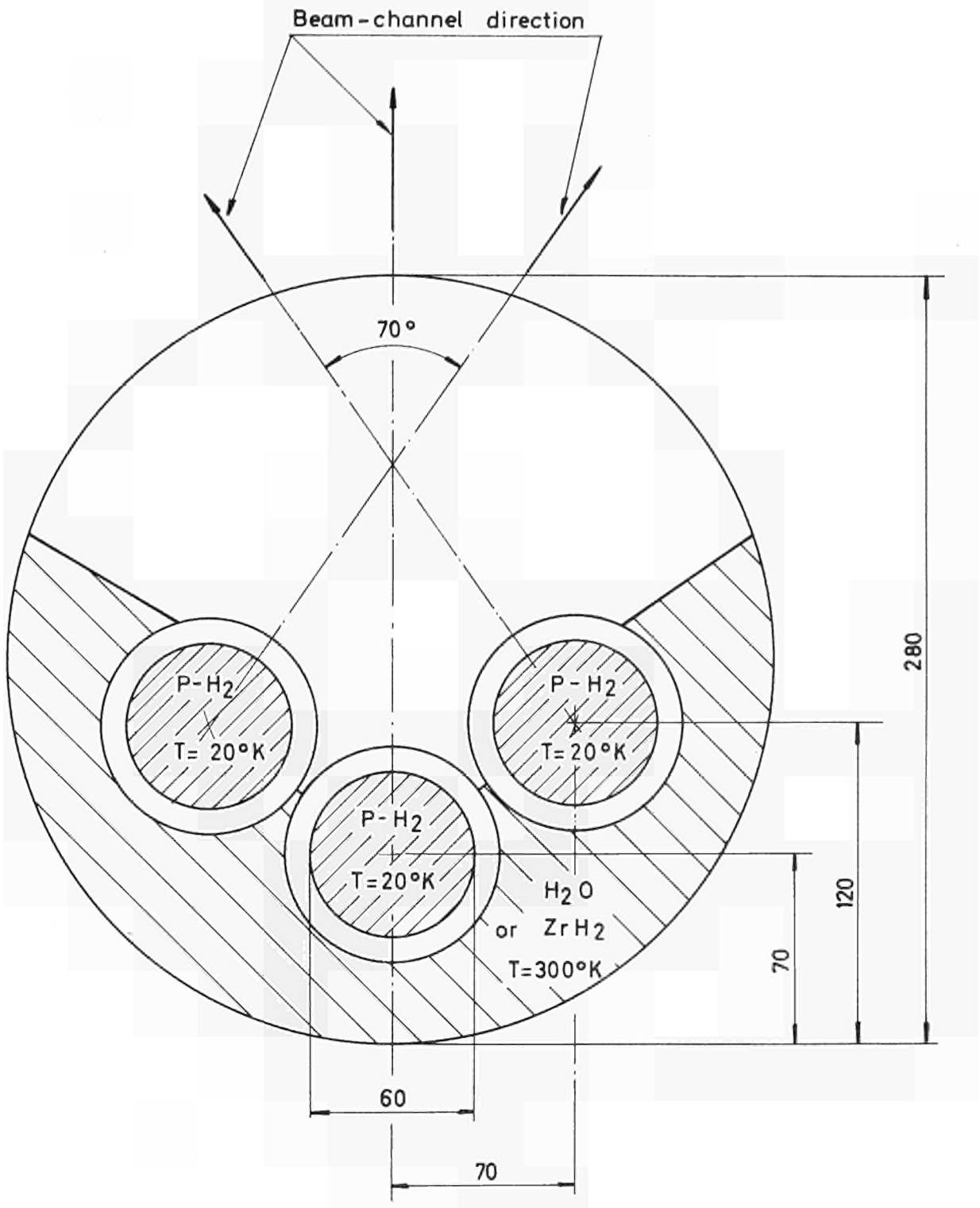

Fig. 14. CONCEPTIONAL DESIGN OF A COLD NEUTRON SOURCE

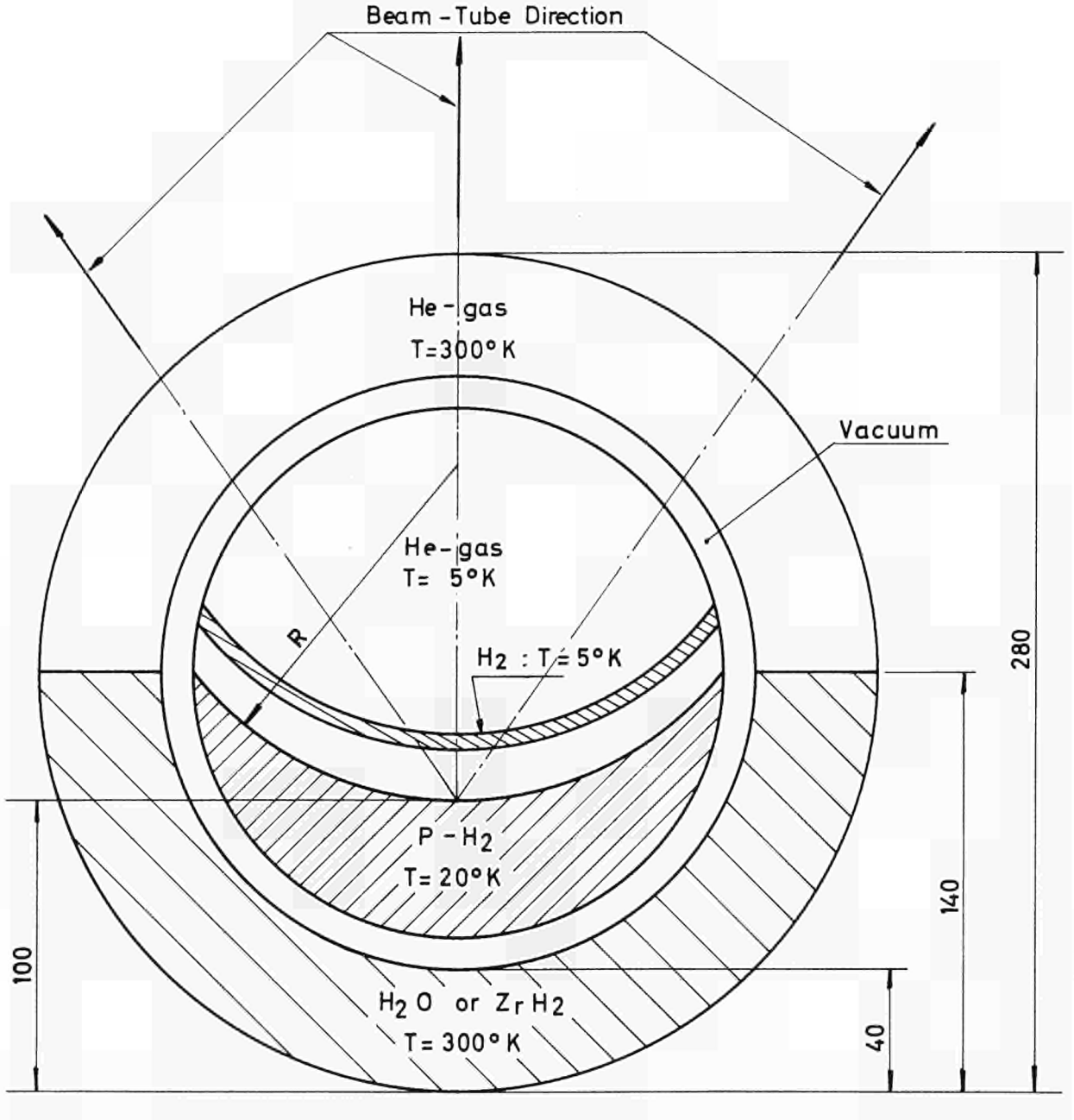

Fig.15. CONCEPTIONAL DESIGN OF A COLD NEUTRON SOURCE

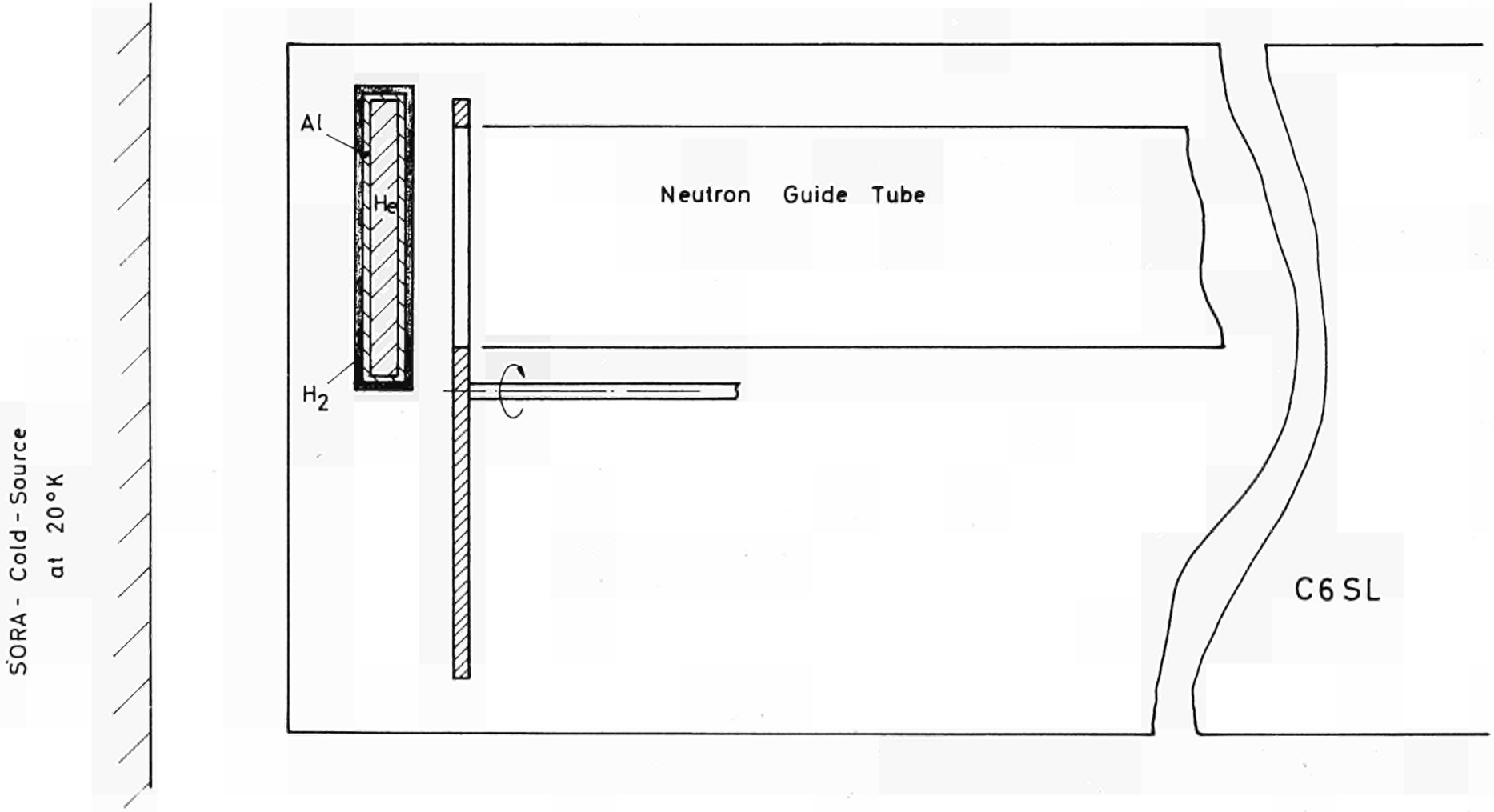

Fig. 16. The conceptional design of the SORA ultra cold neutron source

Fig.17 a Representation of a neutron beam in real and Momentum space

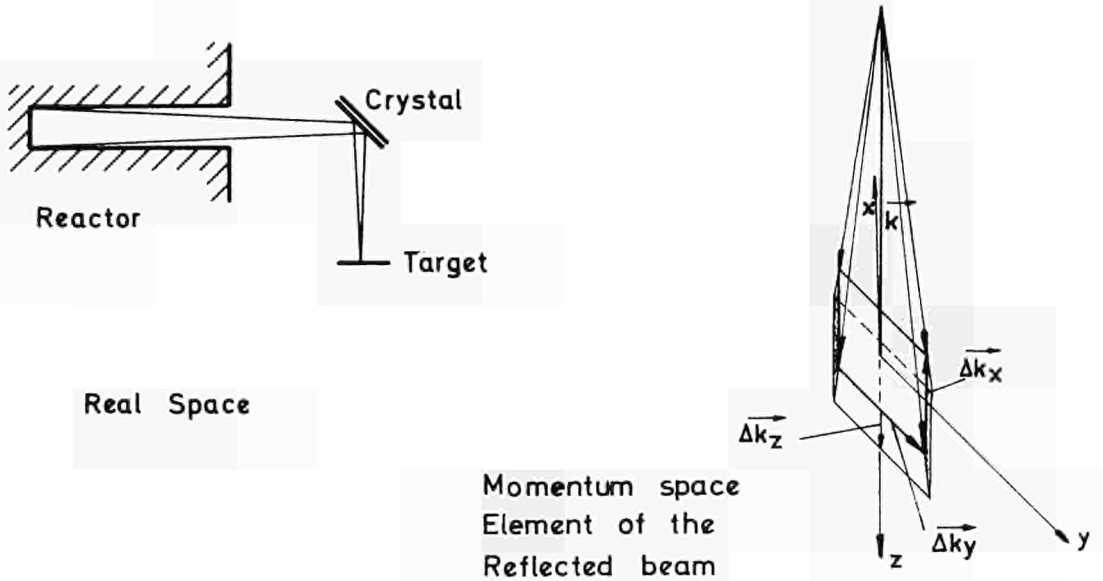

Fig. 17 b Representation of a time of flight experiment in real and Momentum space

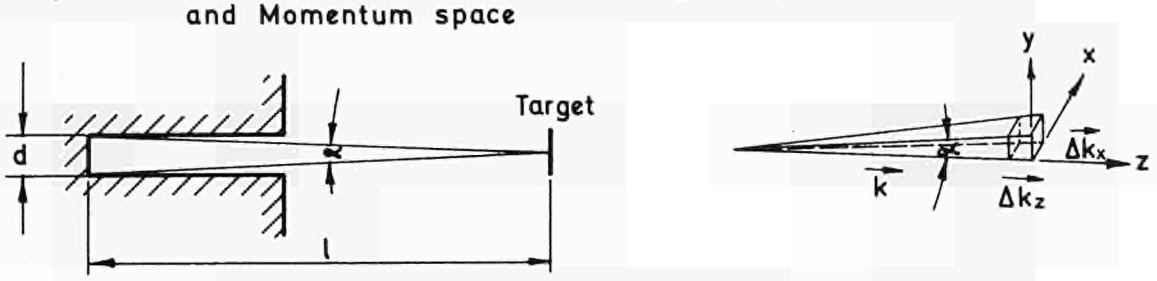

$$\alpha = \frac{d}{l} = \frac{\Delta k_x}{k} \quad ; \quad \frac{\Delta E}{E} = 2\frac{\Delta t}{t} = 2\frac{\Delta t}{l} \cdot v = \frac{2\Delta k_z}{k} \quad ; \quad \Delta t = \frac{d}{v} \cdot \frac{\Delta k_z}{\Delta k_x}$$

Fig. 17 c Elongated Momentum space Element

Fig. 17 d Flat Momentum space Element

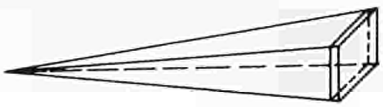

CHARACTERIZATION OF NEUTRON BEAMS IN MOMENTUM SPACE

FIG. 17

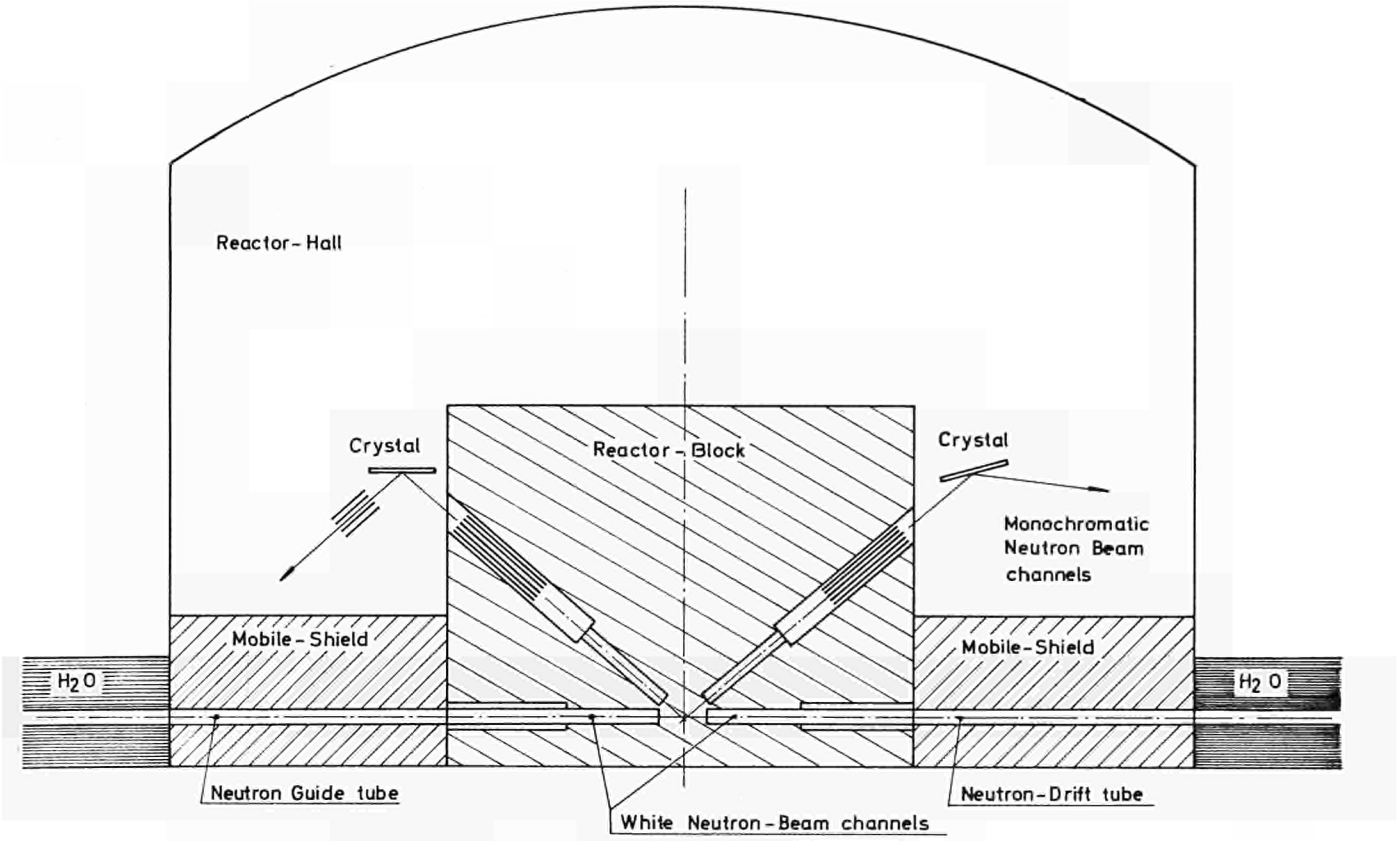

Fig. 18. GENERAL LAY-OUT OF NEUTRON BEAM FACILITIES

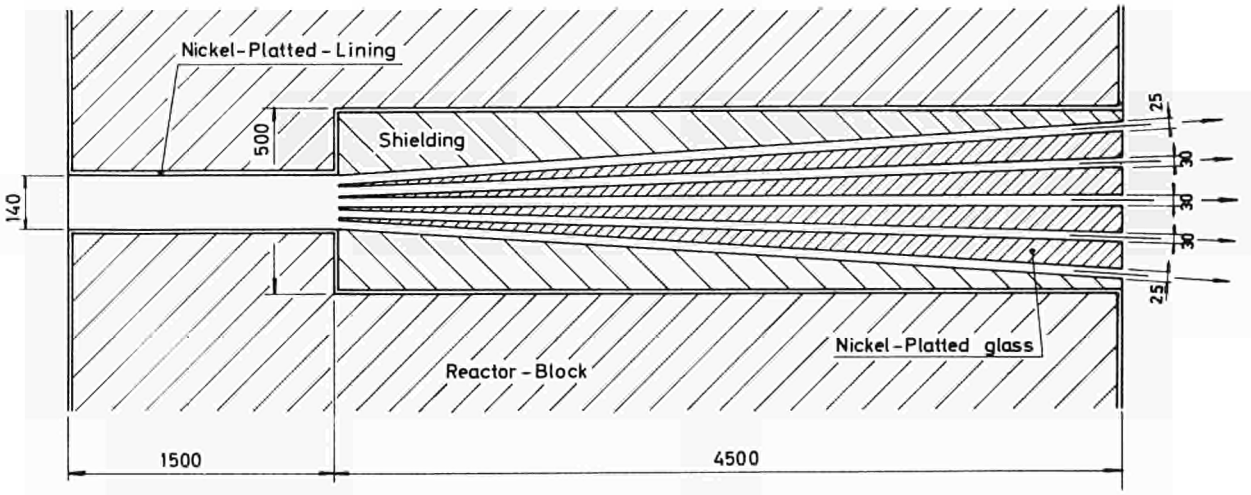

Fig. 19. NEUTRON GUIDE TUBES IN THE SECTION OF THE REACTOR BLOCK

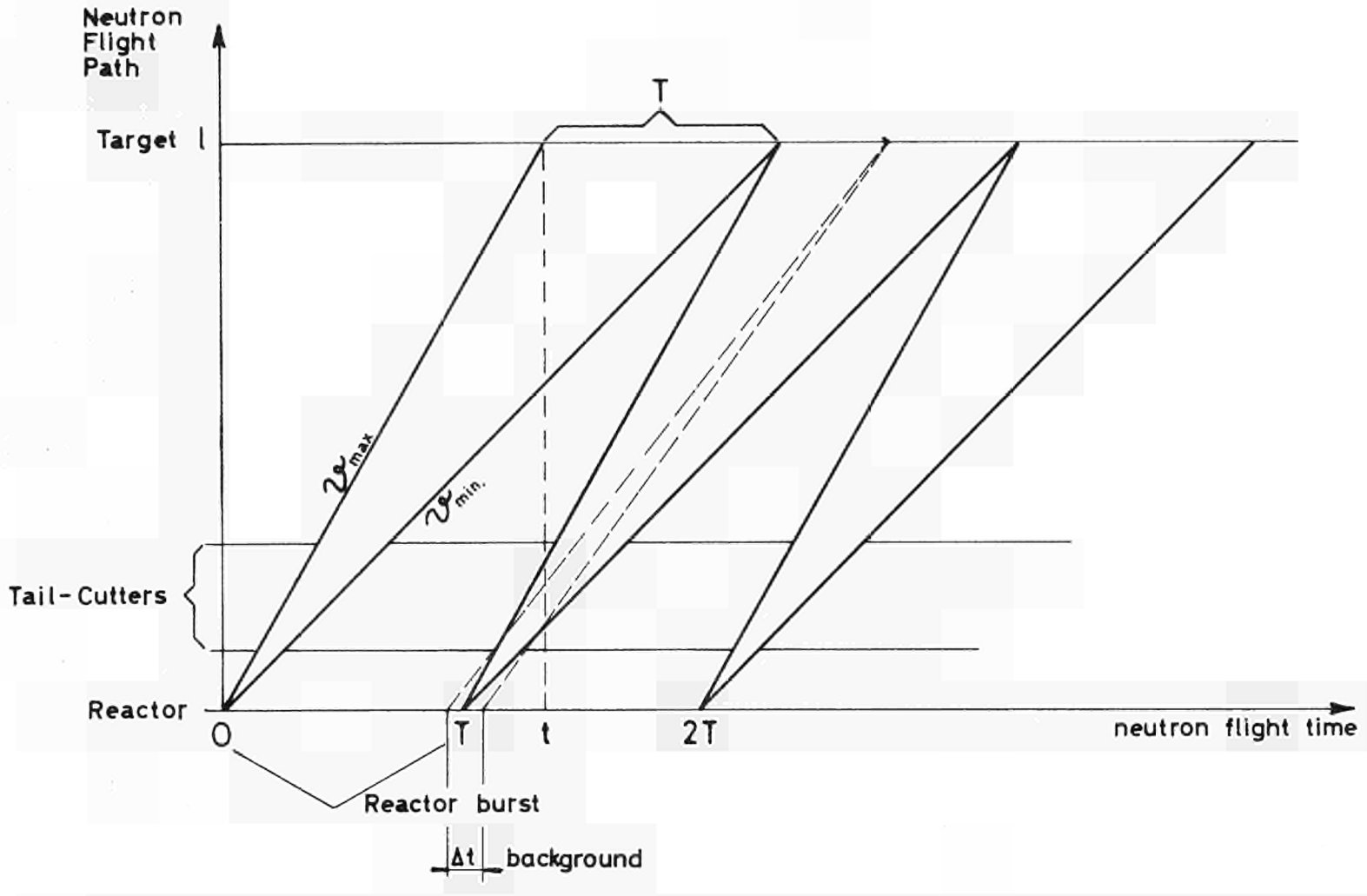

NEUTRON-VELOCITY-BAND-WIDTH-CONDITION FOR A CONTINUOUS QUASI-MONOCHROMATIC BEAM

FIG. 20

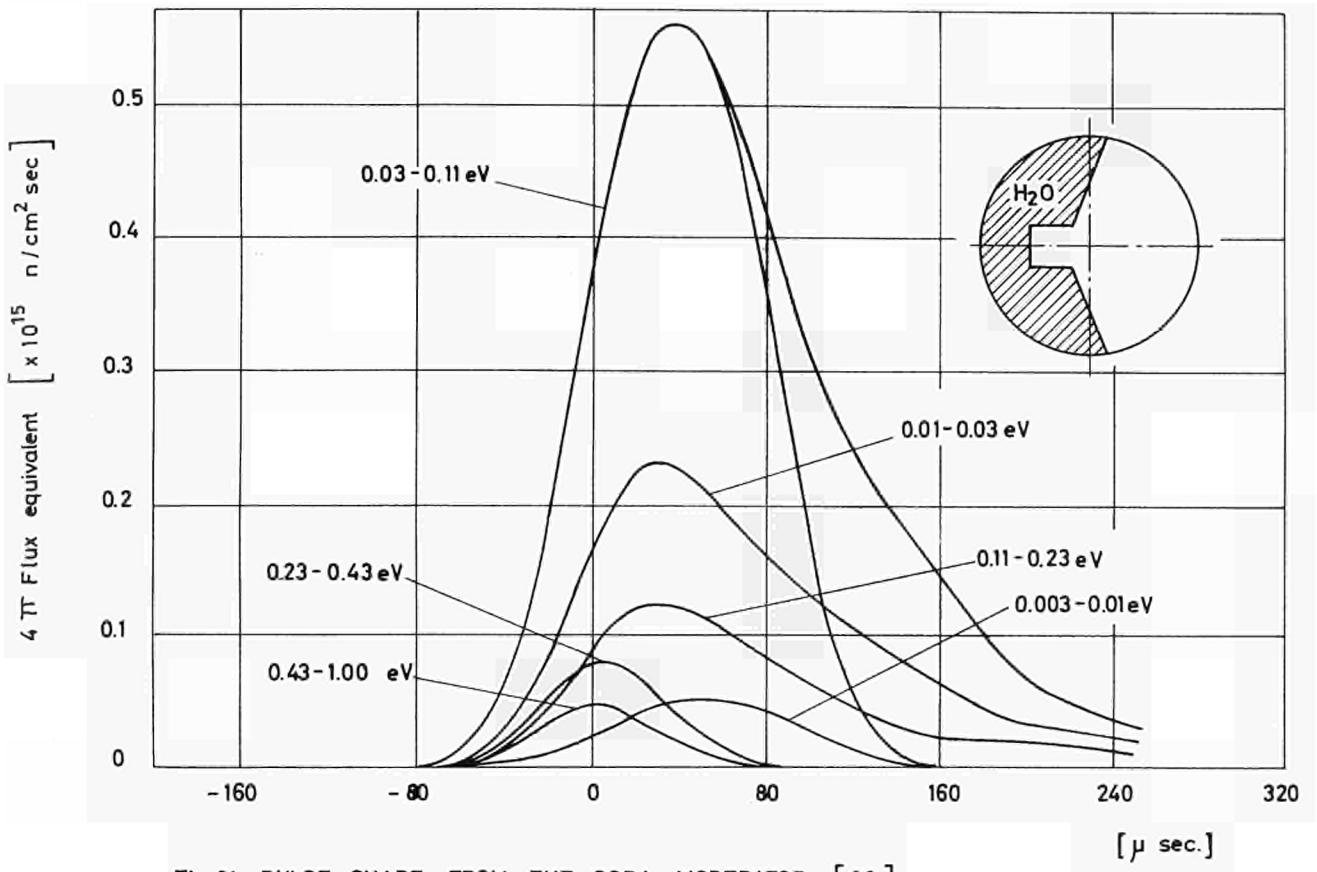

Fig. 21. PULSE SHAPE FROM THE SORA - MODERATOR [22]

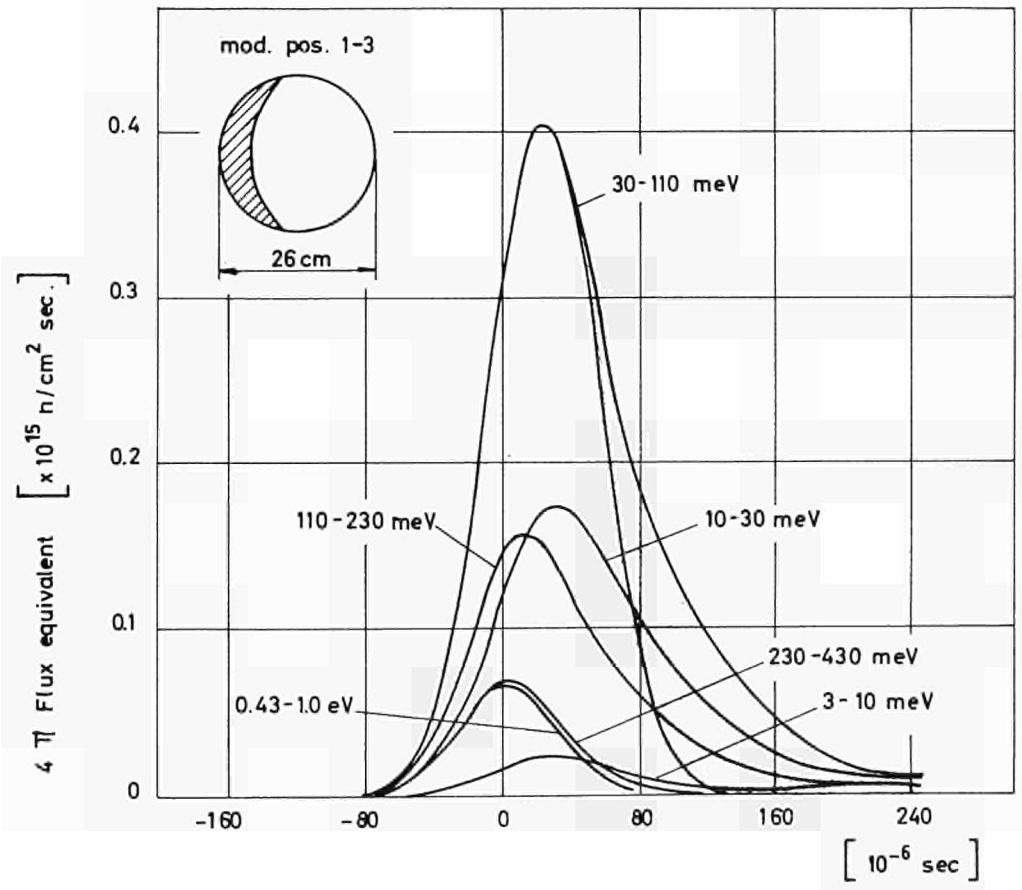

Fig. 22. PULSE SHAPE FROM THE SORA - MODERATOR

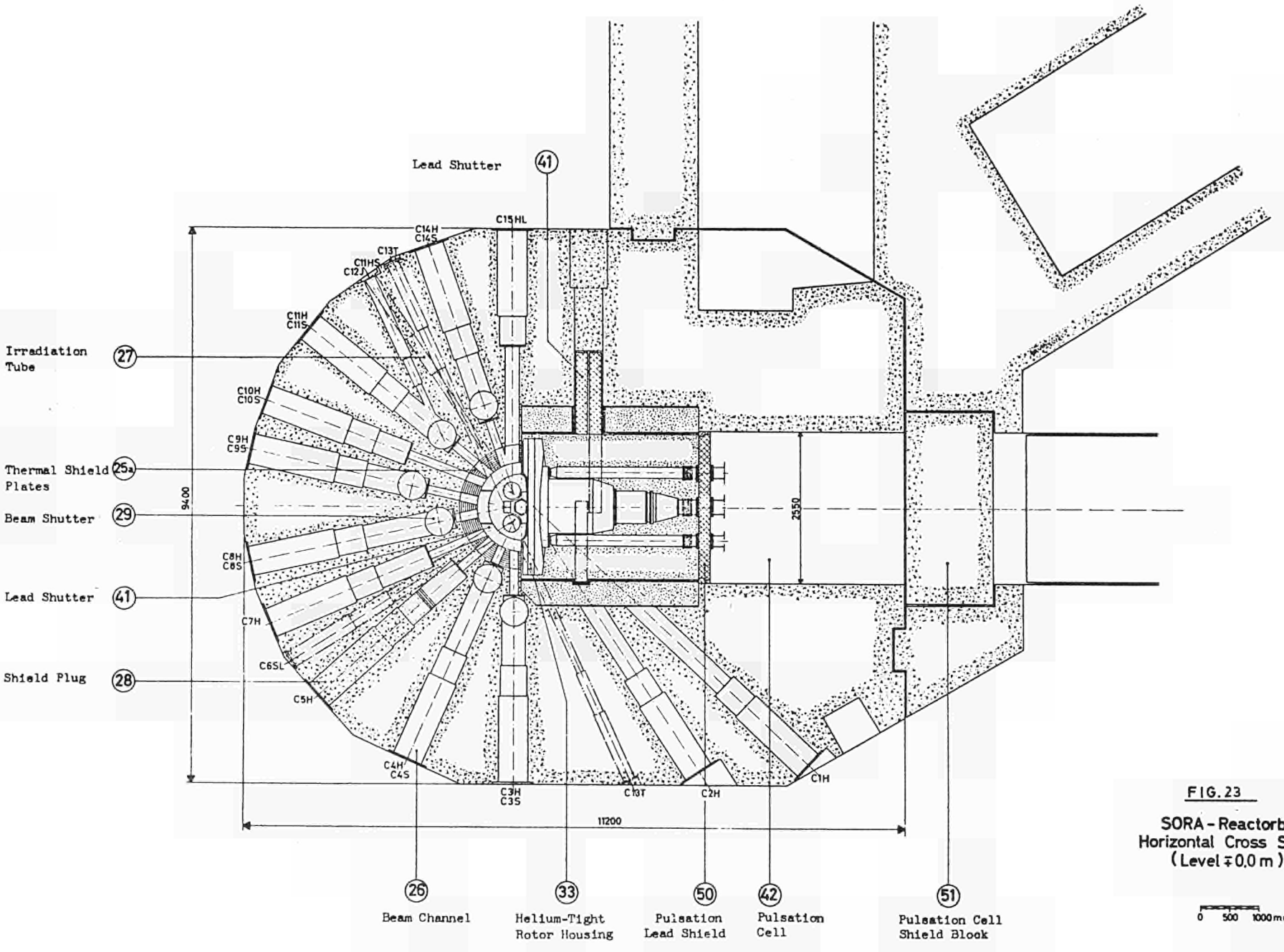

FIG. 23

SORA - Reactorblock
Horizontal Cross Section
(Level ∓0.0 m)

0 500 1000 mm

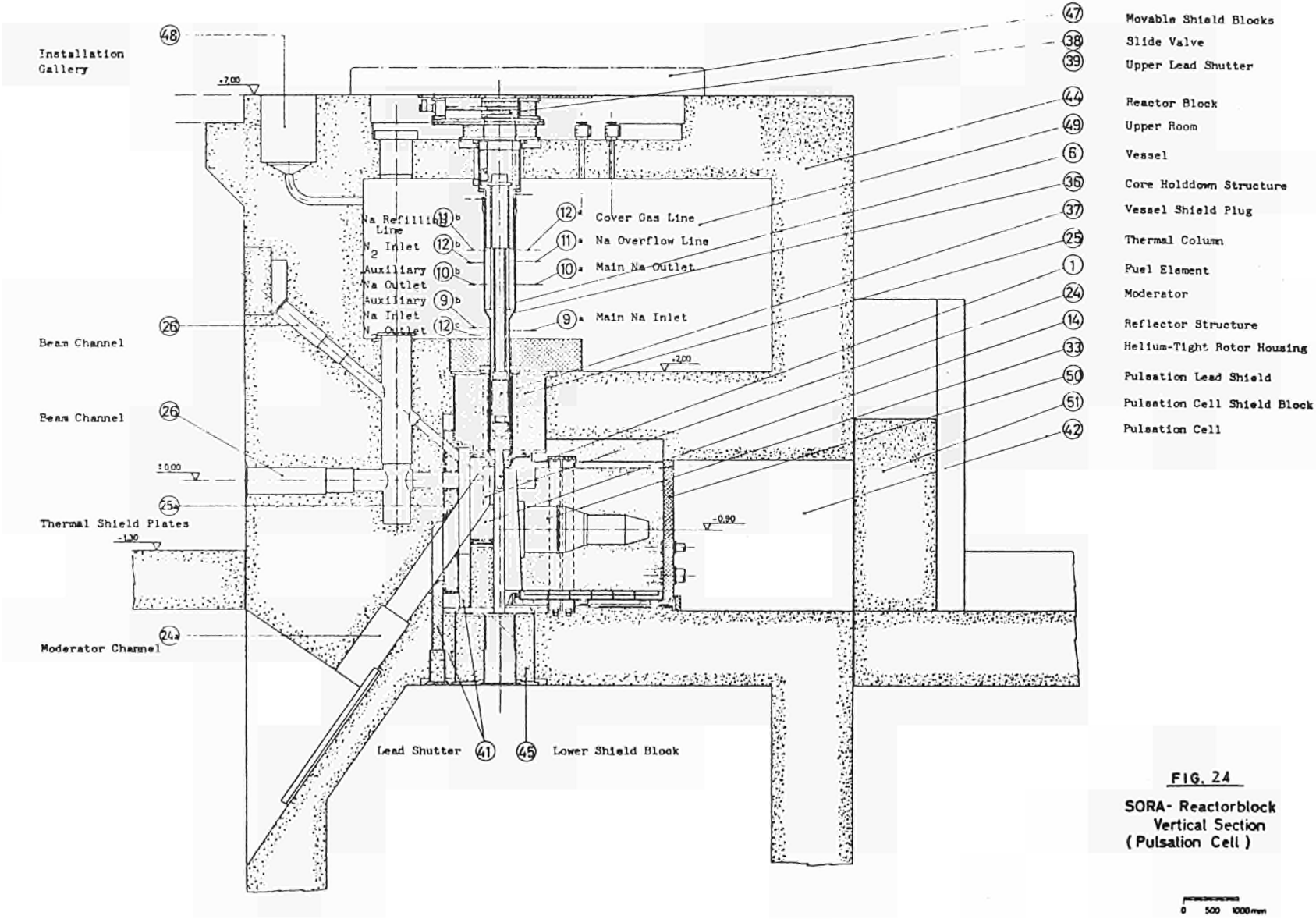

FIG. 24

SORA- Reactorblock
Vertical Section
(Pulsation Cell)

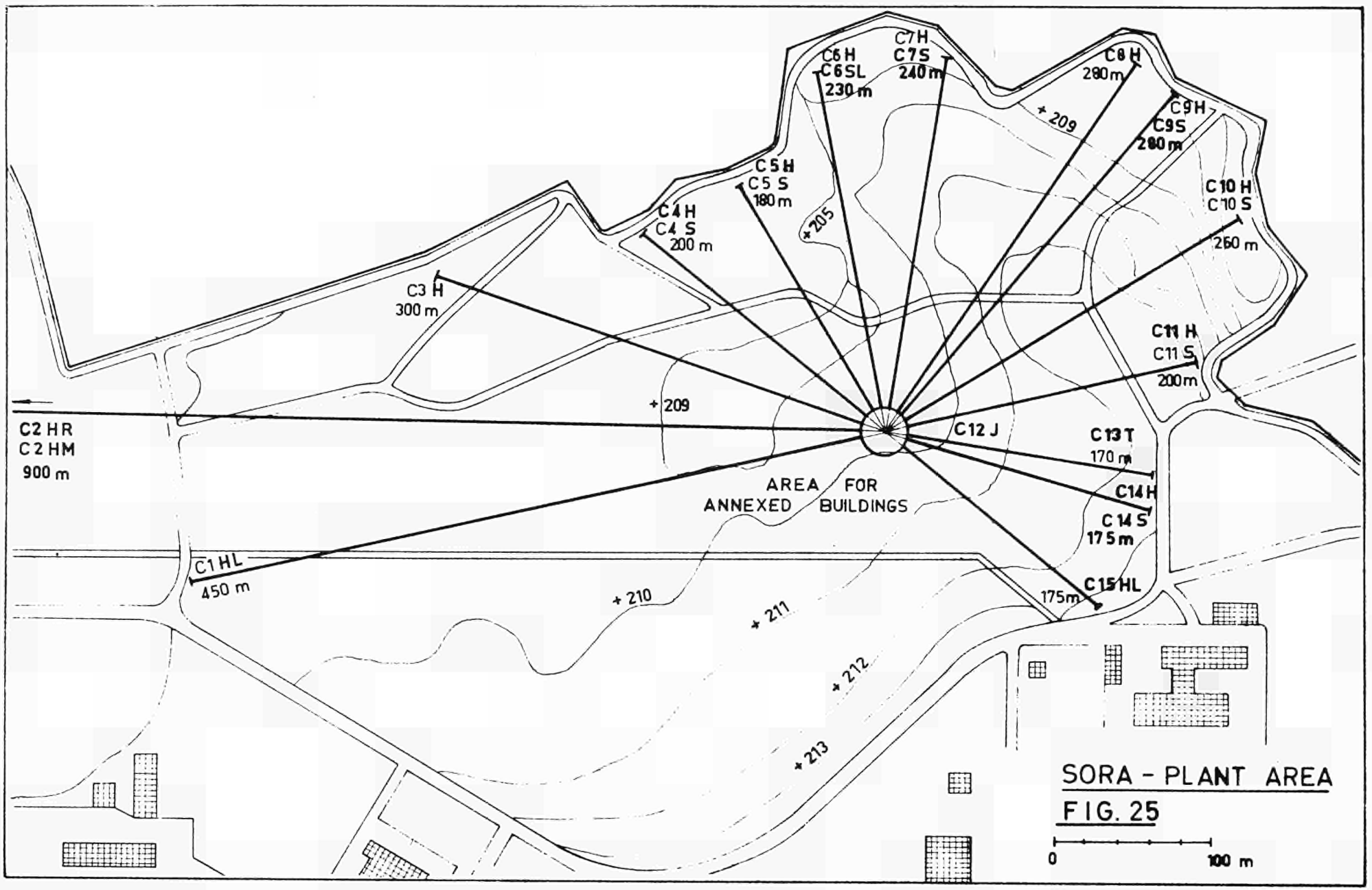
C6 H
C6 SL
230 m
C7 H
C7 S
240 m
C8 H
280 m
C9 H
C9 S
280 m
C10 H
C10 S
260 m
C5 H
C5 S
180 m
C4 H
C4 S
200 m
C3 H
300 m
C11 H
C11 S
200 m
C2 HR
C2 HM
900 m
C12 J
C13 T
170 m
C14 H
C14 S
175 m
C15 HL
175m
C1 HL
450 m
AREA FOR
ANNEXED BUILDINGS
+ 209
+ 205
+ 209
+ 210
+ 211
+ 212
+ 213
SORA - PLANT AREA
FIG. 25
0
100 m

LECTURE II

High Resolution Time of Flight Spectrometry at a Pulsed Neutron Source

I. Introduction

Thermal neutrons have a wave length λ_n comparable to X-rays (λ_x), therefore it has been "natural" to carry over most of the experience and knowledge of X-ray- to neutron-spectroscopy. They propagate with a velocity of v_T = 2200 m/sec, therefore, a second method, the so-called time of flight spectroscopy (TOF), has been established since the beginning of neutron spectroscopy and which is now being carried out with two competing methods using either a continuous or a pulsed neutron source. This situation has stimulated first the development of periodically pulsed fast reactors and boosters at Dubna, U.S.S.R., and at different other places. In the last decade, there have been a number of international conferences on the design aspects and the utilisation of pulsed neutron sources. There it turned out that considerable hesitation and reservation exists towards the use of TOF-spectroscopy and consequently of periodically pulsed neutron sources. Mainly this attitude is taken because one is owner of a continuous reactor and of two and three axis spectrometers or one is lacking full information on the potential of modern TOF-spectroscopy and data handling systems. In the following, I am giving an introduction to the possibilities of modern TOF-spectroscopy that is by far not complete since among others the spectrometers relying on "time focusing" and "space-time-focusing"-effects are not considered at this lecture.

II. Intensity in a Neutron Scattering Experiment

In a neutron scattering experiment the following 4 quantities can be measured:

- the momentum transfer:

$$(1)\quad m\vec{v}_i - m\vec{v}_f = \hbar\vec{k}_i - \hbar\vec{k}_f = \hbar\vec{\varkappa}\,;\ \vec{\varkappa} = \vec{k}_i - \vec{k}_f$$

- the energy transfer:

$$(2)\quad \frac{1}{2}mv_i^2 - \frac{1}{2}mv_f^2 = \frac{\hbar^2}{2m}(k_i^2 - k_f^2) = E_i - E_f = \hbar\omega$$

- the intensity:

$$(3)\quad J \approx d^2\sigma/d\Omega dE \approx S(\vec{\varkappa},\omega) \leftrightarrow F * G(\vec{r},t)$$

$$(4)\quad J \approx d\sigma/d\Omega \approx S(\vec{\varkappa},0) \leftrightarrow F * G(\vec{r},\infty)$$

$$(5)\quad J \approx d\sigma/d\Omega \approx S(\vec{\varkappa}) \leftrightarrow F * G(\vec{r},0)$$

and

- the spin flip probability

$$(6)\quad P = J_f(\downarrow)/J_i(\uparrow).$$

From equation (1) and (2) follows

$$(7)\quad \hbar\omega = \frac{\hbar^2}{2m}\left[2(\vec{\varkappa}.\vec{k}_i) - \varkappa^2\right]$$

which determines a certain trace in the $\varkappa,\omega$-plane for a given k_i. In Fig. 1 the principle features are given for a neutron scattering experiment in real space and in Fig. 2 an example of a neutron scattering experiment in real- and momentum space is given.

According to the notations of Fig. 1, the intensity of a scattering experiment at a pulsed neutron source is given by

$$(8)\ J_{Detector} = \int \frac{1}{4\pi} \Phi(E_i, \Omega_i, t) \cdot dE_i \cdot d\Omega_i \cdot dt \cdot \nu \cdot f_i$$

$$F_T \cdot N \cdot d \cdot \frac{d^2\sigma}{d\Omega_f dE_f}(E_i, \Omega_i, E_f, \Omega_f) \cdot d\Omega_f \cdot dE_f \cdot f_f \cdot \varepsilon(E_f)\ [n/sec]$$

where

$\Phi(E_i, \Omega_i, t)$ is the flux per unit energy and per unit solid angle at the surface of the neutron source at time t

dE_i is the energy spread of the neutrons with energy E_i at the target

$d\Omega_i$ is the solid angle expanded by an area element dF_i of the neutron source area F_s. ($d\Omega_i = dF_i / l_i^2$, where l_i is the distance source-target)

dt the time integration differential

t the time variable

ν the neutron source pulse frequency

f_i is a factor taking into account the intensity loss in the apparatus between the neutron source and the target

F_T is the effective target area (= neutron beam cross section)

N is the atom density of the target material

d is the effective target thickness

$\frac{d^2\sigma}{d\Omega_f dE_f}(E_i, \Omega_i, E_f, \Omega_f) =$

$= \frac{\sigma_s}{4\pi} \cdot \frac{k_f}{k_i} \cdot S(\vec{\varkappa}, \omega)$ is the differential scattering cross section

$\vec{k}_i, \vec{k}_f$ are the initial and final neutron momenta

$\vec{\varkappa} = \vec{k}_i - \vec{k}_f$ is the momentum transfer of the neutron on the target in the scattering process

$\hbar\omega = E_i - E_f$ is the energy transfer of the neutron on the target in the scattering process

$d\Omega_f$ is the solid angle element expanded by an area element dF_f of the neutron detector area F_D ($d\Omega_f = dF_f/l_f^2$, where l_f is the distance target-detector)

dE_f is the energy spread of the neutrons with energy E_f at the detector

f_f is a factor taking into account the intensity loss in the apparatus between the target and the detector

$\varepsilon(E_f)$ is the neutron detector efficiency

If neutrons are scattered coherently from a single crystal, the elastic as well as the inelastic scattering cross section is given in terms of δ-functions and the integration [equation (1)] has to be carried out (integrated intensity).

For all incoherent experiments the cross section is a rather smooth function of $|\vec{\varkappa}|$ and ω and therefore equation (8) can be written according to Maier-Leibnitz [1] in a more simplified manner. The intensity of neutron scattering experiments using time of flight (TOF)-techniques and conventional crystal spectrometry, as outlined in Fig. 3, can be calculated by

$$(9)\quad J_{Detector} = \frac{1}{4\pi} \cdot \Phi(E_i,\Omega_i) \cdot \Delta E_i \cdot \Delta\Omega_i \cdot \Delta t \cdot \nu \cdot f_i \cdot F_T \cdot N \cdot d \cdot \frac{d^2\sigma}{d\Omega_f dE_f} \cdot \Delta\Omega_f \cdot \Delta E_f \cdot f_f \cdot \varepsilon(E_f) \qquad [n/sec]$$

According to Fig. 2

$$(10)\quad \Delta\Omega_i = F_s/l_i^2 = \Delta k_i^{(x)} \cdot \Delta k_i^{(y)}/k_i^2$$

$$(11)\quad \Delta\Omega_f = F_D/l_f^2 = \Delta k_f^{(x)} \cdot \Delta k_f^{(y)}/k_f^2$$

$$(12)\ \frac{\Delta E_i}{E_i} = 2\frac{\Delta k_i}{k_i}\ ;\ \frac{\Delta E_f}{E_f} = 2\frac{\Delta k_f}{k_f}$$

$$(13)\ \Delta E_i = \frac{\hbar^2}{2m} \cdot k_i \cdot \Delta k_i^{(z)}\ ;\ \Delta E_f = \frac{\hbar^2}{2m} \cdot k_f \cdot \Delta k_f^{(z)}$$

$$(14)\ \Delta V_i = \Delta k_i^{(x)} \cdot \Delta k_i^{(y)} \cdot \Delta k_i^{(z)} \cdot \hbar^3$$

$$(15)\ \Delta V_f = \Delta k_f^{(x)} \cdot \Delta k_f^{(y)} \cdot \Delta k_f^{(z)} \cdot \hbar^3$$

and since for a scalar flux

$$(16)\ \Phi(E_i, \Omega_i) = \Phi_{total} \cdot e^{-E_i/E_T} \cdot \frac{E_i}{E_T} \cdot \frac{\Delta E_i}{E_T}$$

and furthermore

$$(17)\ E_T = k_B \cdot T = \frac{\hbar^2}{2m} k_T^2\ ;\ E_i = \frac{\hbar^2}{2m} k_i^2\ ;\ E_f = \frac{\hbar^2}{2m} k_f^2$$

$$(18)\ \vec{\varkappa} = \vec{k}_i - \vec{k}_f\ ;\ \hbar\omega = E_i - E_f = \frac{\hbar^2}{2m}(k_i^2 - k_f^2)$$

we can rewrite equation (9)

$$(19)\ J_{Detector} = A(T) \cdot f_i \cdot F_T \cdot N \cdot d \cdot \sigma_s \cdot \rho(\vec{\varkappa}, \omega) \cdot f_f \cdot \Delta V_i \cdot \Delta V_f \cdot \varepsilon(E_f)\ [n/sec]$$

where

$$(20)\ A(T) = \frac{\Phi_{total}}{8\pi^2 mh^4} \cdot \frac{e^{-k_i^2/k_T^2}}{k_T^4} = \frac{1}{4\pi m^2}\ \rho(T)$$

and

$$(21)\ \rho(T) = \frac{\Delta n}{\Delta V_i} = \frac{\Phi_{total}}{2\pi} \cdot \frac{m}{\hbar^4} \cdot \frac{e^{-k_i^2/k_T^2}}{k_T^4} \cdot$$

$\rho(T)$ stands for the neutron density in momentum space. The intensity at the target and the detector is therefore proportional to

$$(22)\quad J_{Target} \approx \frac{e^{-k_i^2/k_T^2}}{k_T^4} \cdot \Delta V_i$$

$$(23)\quad J_{Detector} \approx \rho(\vec{x}, \omega) \cdot \frac{e^{-k_i^2/k_T^2}}{k_T^4} \cdot \Delta V_i \cdot \Delta V_f$$

In a TOF-experiment as illustrated in Fig. 3, where the collimation or $\Delta\Omega_i$ is the same for all k_i, the momentum space volume ΔV_i is proportional to k_i^4 since

$$(24)\quad \frac{\Delta k_i^{(z)}}{k_i} = \frac{\Delta t}{t} = \frac{\Delta t}{l_i} \cdot v_i = \left[\frac{\Delta t}{l} \cdot \frac{h}{m}\right] \cdot k_i = \text{const.} k_i$$

and

$$(25)\quad \Delta\Omega_i = \Delta k_i^{(x)} \cdot \Delta k_i^{(y)} / k_i^2$$

and therefore

$$(26)\quad \Delta V_i \approx \Delta\Omega_i \cdot k_i^4 .$$

The intensity at the target is therefore proportional to

$$(27)\quad J_{Target} \approx \frac{e^{-k_i^2/k_T^2}}{k_T^4} \cdot k_i^4 = e^{-E_i/E_T} \cdot \left(\frac{E_i}{E_T}\right)^2 = e^{-X} \cdot X^2$$

In Fig. 4 the relative intensity at the position of the target is plotted as a function of $x = E_i/E_T$. It can be seen that the intensity is a slowly varying function in a rather large energy range. Since in any neutron scattering experiment the resolution has to be adjusted to the neutron source strength, the TOF-technique is an appropriate method for diffraction and neutron down-scattering experiments.

It has been assumed that Δt is constant for all neutron energies, an as-

sumption only valid for choppers and approximately valid for periodically pulsed reactors. A detailed discussion on the energy resolution functions and the accessibility in the $\varkappa,\omega$ plane of inverted spectrometers is given elsewhere by W. Kley and W. Matthes [2].

III. Momentum Space Diagrams

III. 1. Momentum Space Diagrams for Elastic Scattering at Perfect and Imperfect (Mosaic) Crystals

In Fig. 5. a, 5. b and 5. c the production of monochromatic neutron beams by reflection from a perfect crystal, a crystal with a continuous variable lattice spacing and an imperfect (mosaic) crystal is shown in real- and momentum space representation.

III. 2. Momentum Space Diagrams for Coherent Inelastic Neutron Scattering Experiments

From Fig. 6. a follows

$$(28)\quad \frac{\hbar^2}{2m}(\underset{\sim}{k}_i^2-\underset{\sim}{k}_f^2)=\frac{\hbar^2}{2m}(l_i^2-l_f^2)=\pm\hbar\omega(\vec{q})=E_i-E_f$$

$$(29)\quad \vec{\underset{\sim}{k}}_i-\vec{\underset{\sim}{k}}_f=\vec{\varkappa}=2\pi\vec{\tau}\pm\vec{q}$$

where the upper sign stands for phonon emission and the lower one for phonon absorption. k_i and k_f are the mean wave vector of the incoming and scattered neutrons. For the derivation of the focusing condition for a TOF-experiment, we follow now the method developed by Kalus [3] for triple axis spectrometry. From Fig. 6. a follows that for all vectors $\vec{k}_i$ and $\vec{k}_f$ that are lying on a plane P, perpendicular to $\vec{K}$ and within the volume elements ΔV_i and ΔV_f the momentum-energy-relation for phonon scattering is fulfilled. Fig. 6. b gives the usual momentum space representation of neutron beams where all the points of the $\vec{k}_i$ and $\vec{K}_f$ vectors are joint in one point and the momentum-energy-relation for

phonon scattering is fulfilled for all vectors $\vec{k}_i$ and $\vec{k}_f$ lying on planes P_i, P_f parallel to the plane P. But also neighbouring vectors $\vec{k}_i + \Delta\vec{k}_i$ and $\vec{k}_f + \Delta\vec{k}_f$ fulfill the momentum-energy-relation in first order approximation if the following relations are fulfilled:

$$(30)\quad 2\,\vec{k}_i \cdot \Delta\vec{k}_i - 2\,\vec{k}_f \cdot \Delta\vec{k}_f = \pm \frac{2m}{h}\,\Delta\omega(\vec{q}) = \pm \frac{2m}{h}\,\mathrm{grad}\,\omega(\vec{q}) \cdot \Delta\vec{q}$$

$$(31)\quad \Delta\vec{k}_i - \Delta\vec{k}_f = \pm\Delta\vec{q}$$

From equation (28) - (31) follows

$$(32)\quad \left\{ \vec{k}_i - \frac{m}{h}\,\mathrm{grad}\omega(\vec{q}) \right\} \cdot \Delta\vec{k}_i = \left\{ \vec{k}_f - \frac{m}{h}\,\mathrm{grad}\omega(\vec{q}) \right\} \cdot \Delta\vec{k}_f = C_\nu$$

Assuming that the single crystal is oriented in such a way that $\mathrm{grad}\,\omega(\vec{q})$ is lying in the scattering plane, then equation (32) defines planes in momentum space that are perpendicular to the vectors $(\vec{k}_i - \frac{m}{h}\,\mathrm{grad}\,\omega)$ and $(\vec{k}_f - \frac{m}{h}\,\mathrm{grad}\,\omega)$. A certain value of C_ν defines two planes W_ν^i and W_ν^f in such a way that all vectors $\vec{k}_i$ and $\vec{k}_f$ lying on the corresponding planes are fulfilling the momentum-energy-relation for phonon scattering. A set of C_ν-values generates pairs of corresponding planes W_ν^i and W_ν^f. Neutrons with $\vec{k}_i$-values lying in the momentum space element, defined by the planes W_o^i and W_1^i, can not be scattered into momentum space elements defined by W_ν^f and $W_{\nu+1}^f$ excepts for $\nu=0$. This is equivalent to the construction of the well-known scattering plane in first order approximation.

With the help of this momentum space diagram technique we can derive immediately the focusing condition for time of flight spectroscopy. Since in time of flight spectroscopy using pulsed neutron sources (not choppers) the momentum space elements are perpendicular to $\vec{k}_i$, see Fig. 7, and consequently we have to orient the crystal in such a way that the vector $\frac{m}{h}\,\mathrm{grad}\,\omega$ is collinear with $\vec{k}_i$.

The orientation of the corresponding momentum space elements for the appropriate $\vec{k}_f$ values is then fixed. If time of flight techniques (choppers and statistical choppers) are also used for the analysis of the scattered neutron beam $(\vec{k}_f)$, then the orientation of the detector area is fixed too in order to obtain focusing condition. As indicated in Fig. 7, neutrons from the same momentum space element are all arriving at the same time at the detector in spite of their different neutron velocities. Note that for the final momentum space elements the shape characteristic for choppers has been used.

In Fig. 7. b the main features of a TOF-experiment in focusing condition is given together with a neutron-trajectory-time-table.

IV. The Mono-Energetic-Neutron-Beam-Facilities

As already outlined in Lecture I, the monoenergetic-neutron-beam facilities ought to be installed at the slanted beam tubes of a pulsed neutron source. Pulsed neutron sources have relative low mean power, consequently large beam tubes ($\varnothing \approx$ 30 cm) can be installed. As shown in Fig. 8. a, the initial neutron energy is defined by classical double crystal spectrometer technique with a large beam cross section. The scattered neutrons are analysed by time of flight techniques. The pulse duration of the monoenergetic neutrons impinging on the sample is given by

$$(33)\quad \Delta t(v_i) = \left\{ \Delta t_M(v_i) + \left(\frac{l_i}{v_i}\right)^2 \cdot \left(\frac{\Delta v_i}{v_i}\right)^2 \right\}^{1/2}$$

where $\Delta t_M(v_i)$ is the pulse duration of the neutron source, v_i the initial neutron velocity, l_i the distance between neutron source and target and $\Delta v_i / v_i$ the neutron velocity resolution of the double crystal spectrometer. The spectrometer is particularly suitable for all incoherent down-scattering experiments with large momentum- and large and small energy transfer with moderate accuracy (% range).

Fig. 8.b is an example of a small sample high resolution spectrometer using a statistical chopper ($\Delta t \approx$ some μsec). [4-8].

V. The White Neutron Diffraction Spectrometer

Simultaneous determination of complex structures and their dynamical properties (elastic force constants) are of interest. Fig. 9 gives examples for Debye-Scherrer and Laue-Spectrometers. The application of a statistical chopper in a white neutron beam, as proposed first by Kley [5, 6], allows to obtain a very good signal to background ratio and the measurement of elastic as well as weak inelastic lines at the same time.

VI. High Resolution White Neutron Beam Spectrometers for Inelastic Scattering Experiments

As outlined in chapter III, the TOF-technique can be used in an as flexible manner as the conventional triple axis spectrometer. Fig. 10 gives various examples. The energy band of the impinging neutron beam can be changed by changing the phase conditions of the overlap rotors, the single crystal (target) can be oriented at will (e.g.: $\frac{m}{\hbar} \operatorname{grad} \omega(\vec{q})$ collinear with k_i), as well as the position and orientation of the detectors.

Fig. 11 gives examples for elastic and inelastic small angle scattering experiments using very cold neutrons. ($T_M \cong 5^{\circ}K$, H_2- or CH_4-moderators).

VII. Literature

1. Maier-Leibnitz, H., Nukleonik, 8, 61,(1966)

2. Kley, W., Matthes, W., EUR-Report in print

3. Kalus, J., Z. Physik 254, 148-161 (1972)

4. Króo, N., Panel Conference on Instrumentation for Neutron Inelastic Scattering, I.A.E.A., Vienna, (1970)

5. Kley, W., July 14th (1971), SORA-Programm; not available

6. Kley, W., EUR-Report No. 4954 e, Proceedings of Joint Meeting EURATOM-Japan Atomic Energy Society, Ispra, Sept. 17-18, (1971)

7. Matthes, W., I.A.E.A.-Proceedings Symposium, Grenoble, Neutron Inelastic Scattering, March 6-10, (1972), p. 773

8. Króo, N., Pellionisz, Vizi, I., Zsigmond, G., Zhukov, G., Nagy, G., I.A.E.A.-Proceedings Symposium, Grenoble, Neutron Inelastic Scattering, March 6-10 (1972), p. 763

VIII. Figure Captions

Fig. 1 Geometrical Representation of a Neutron Scattering Experiment

Fig. 2 A Neutron Scattering Experiment with Monochromatic Neutron Beams in Real- and Momentum-Space

Fig. 3 The Inverted Statistical Chopper Facility

Fig. 4 The Relative Intensity at the Target as a Function of the Relative Neutron Energy $x = E_i/E_T$.
$E_T = k_B . T$ (k_B = Boltzmann-Constant, T = Moderator-Temperature)

Fig. 5 Momentum Space Diagrams for Elastic Scattering

Fig. 6.a Momentum Space Diagram for Phonon Scattering

Fig. 6.b Focusing Condition for Phonon Scattering

Fig. 7.a Focusing Condition for Time-of-flight Phonon-Spectroscopy

Fig. 7.b The Main Features of a TOF-Experiment in Focusing Condition

Fig. 8 The Mono-Energetic-Beam Facilities at the Hot, Thermal and Cold Neutron Source

Fig. 9 The White Neutron Diffraction Spectrometers for the Hot, Thermal and Cold Neutron Source

Fig. 10 High Resolution Spectrometers for inelastic scattering Experiments

Fig. 11 The Very Cold Neutron Facilities

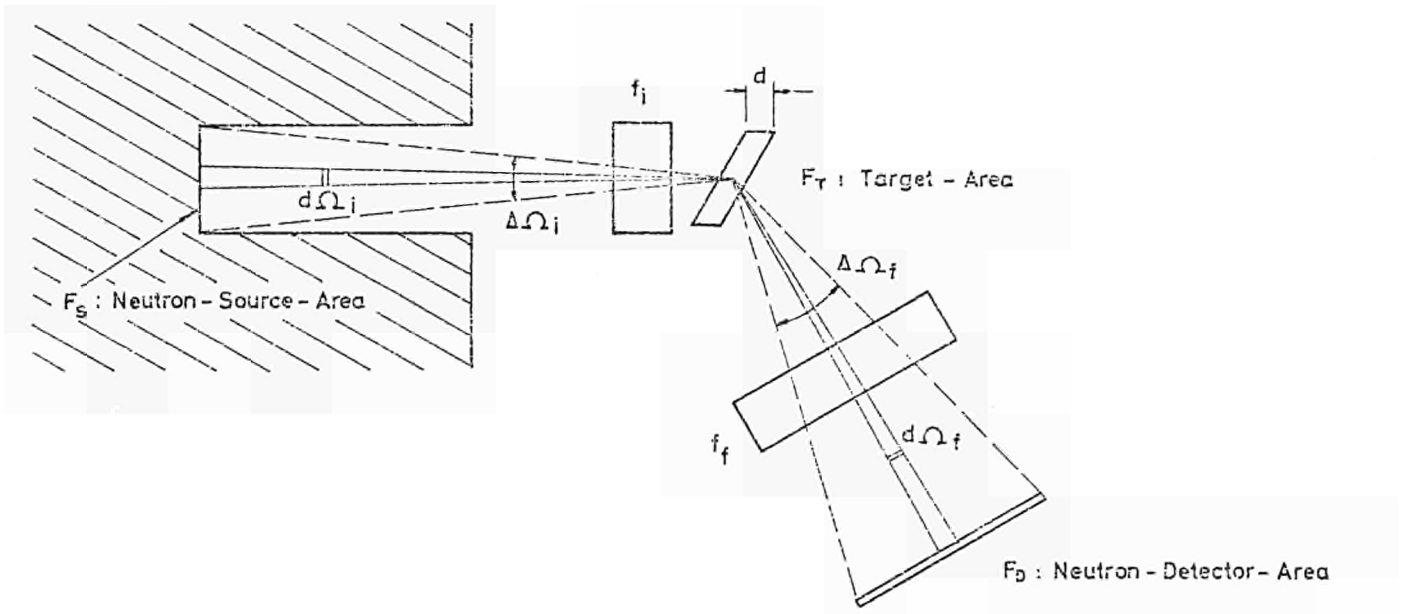

Fig. 1 GEOMETRICAL REPRESENTATION OF A NEUTRON SCATTERING EXPERIMENT

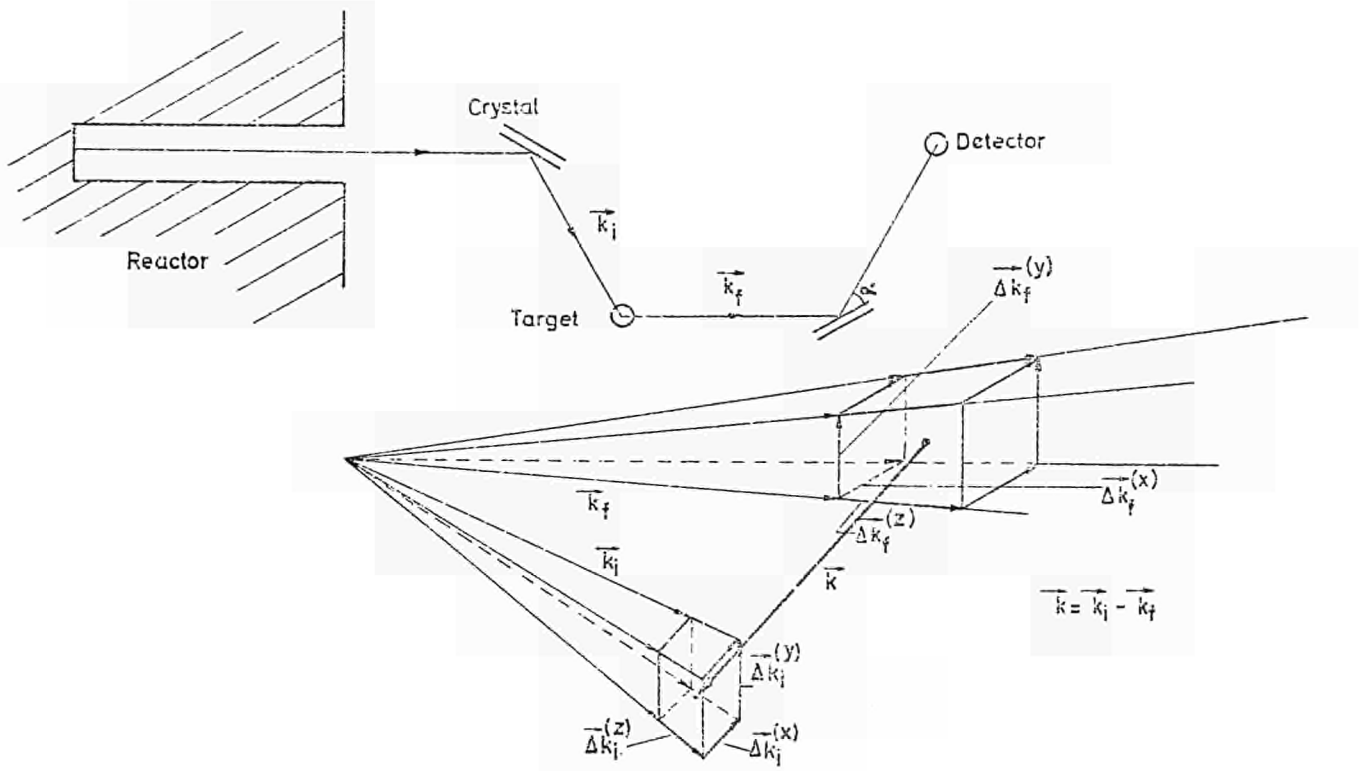

Fig. 2. A NEUTRON SCATTERING EXPERIMENT WITH MONOCHROMATIC NEUTRON BEAMS IN REAL- AND MOMENTUM-SPACE

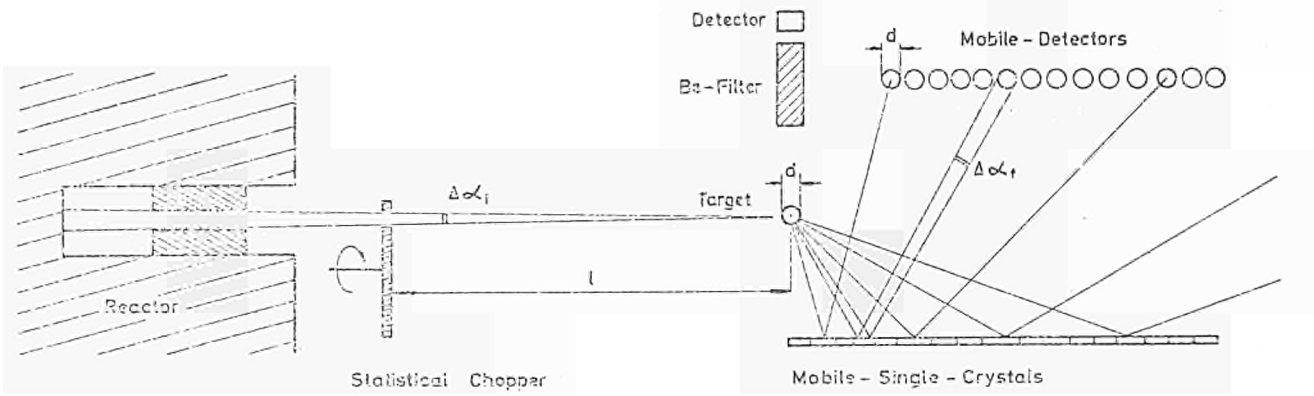

Fig. 3. THE INVERTED STATISTICAL CHOPPER FACILITY

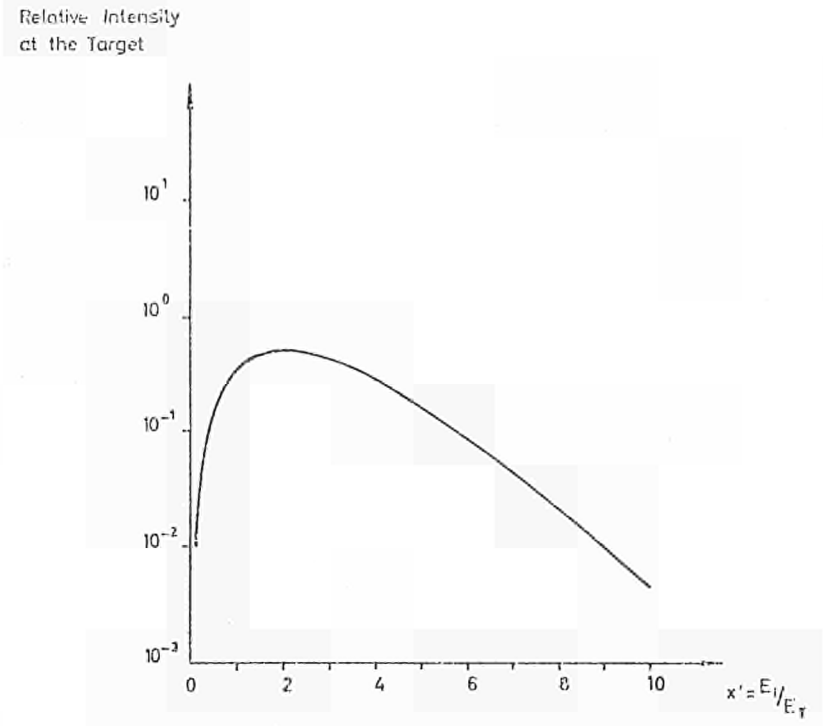

Fig. 4. THE RELATIVE INTENSITY AT THE TARGET AS A FUNCTION OF THE RELATIVE NEUTRON ENERGY $x' = E_i/E_t$

$E_T = K_B \cdot T$ (K_B = Boltzmann - Constant ; T = Moderator-Temperature)

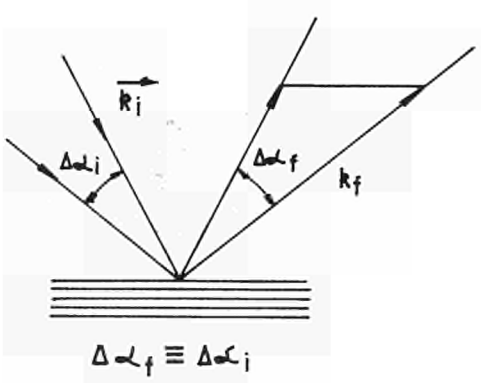

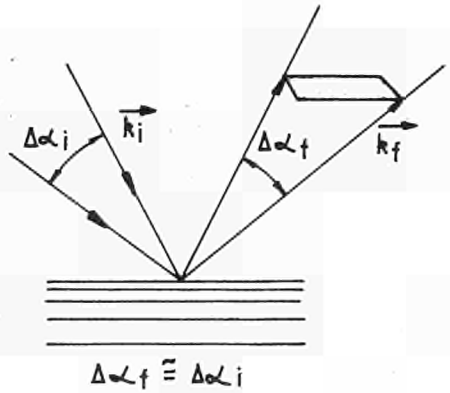

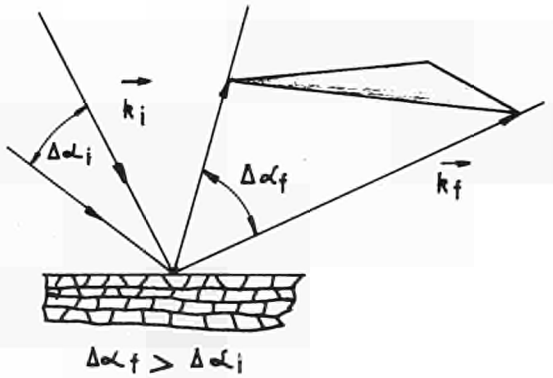

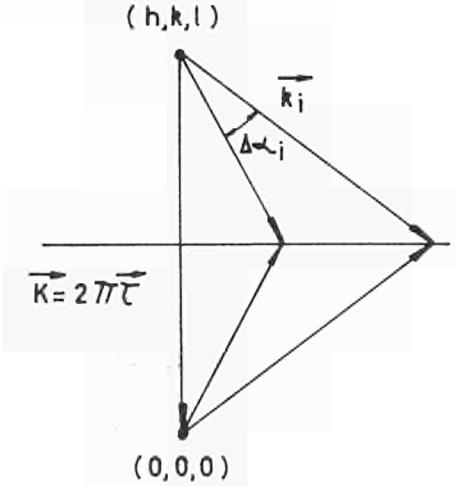

Fig. 5.a. Perfect Crystal

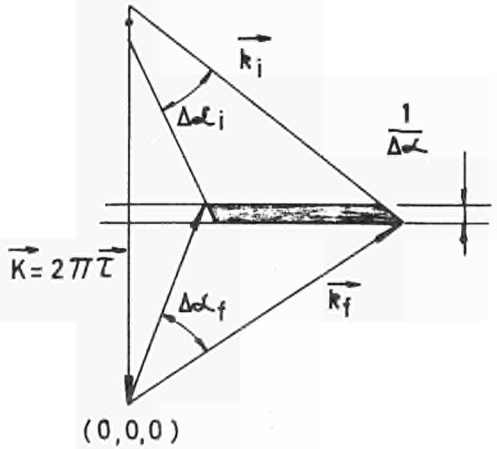

Fig. 5.b. Crystal with Variable Lattice Spacing

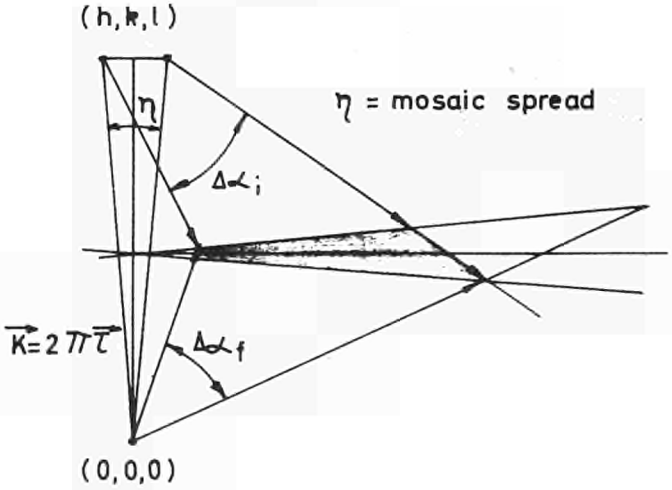

Fig. 5.c Mosaic Crystal

Fig. 5 MOMENTUM SPACE DIAGRAMS FOR ELASTIC SCATTERING

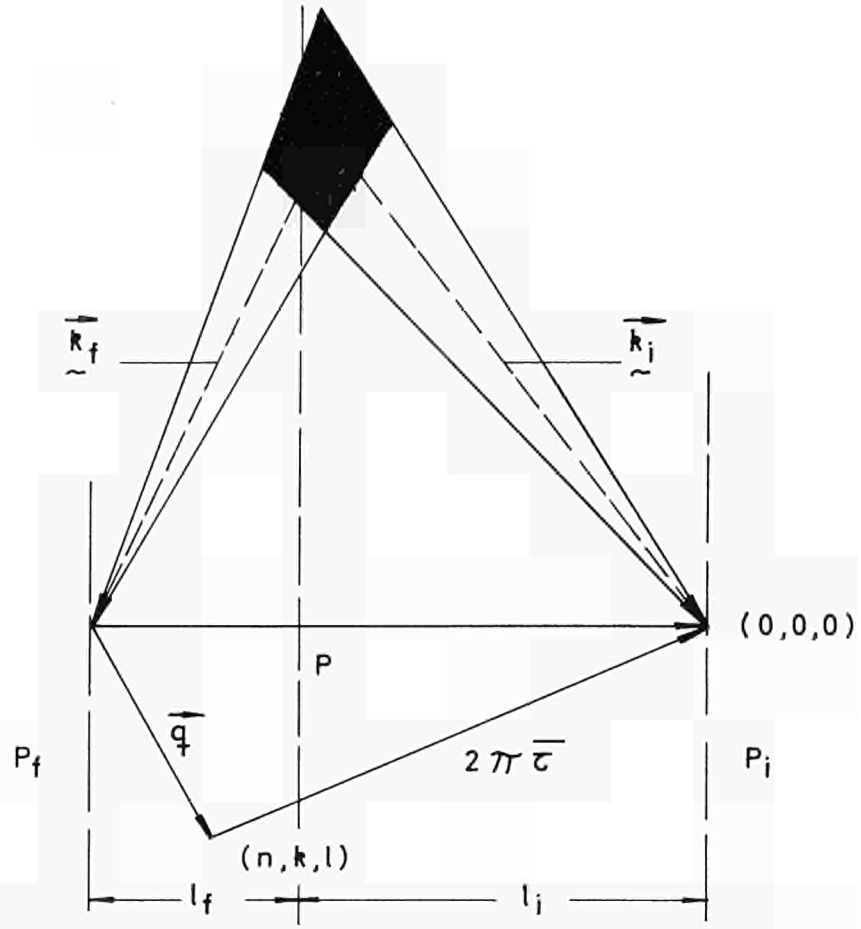

Fig. 6.a. MOMENTUM SPACE DIAGRAM FOR PHONON SCATTERING

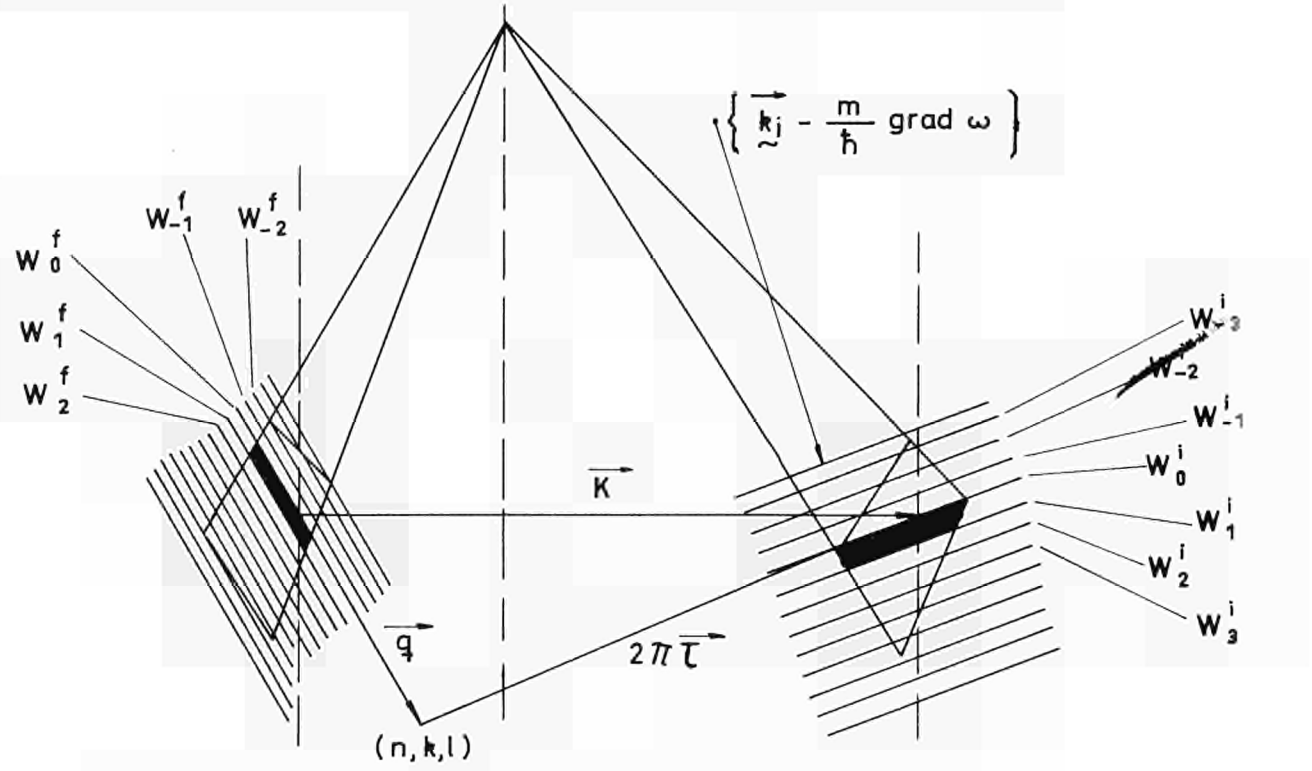

Fig. 6b. FOCUSING CONDITION FOR PHONON SCATTERING

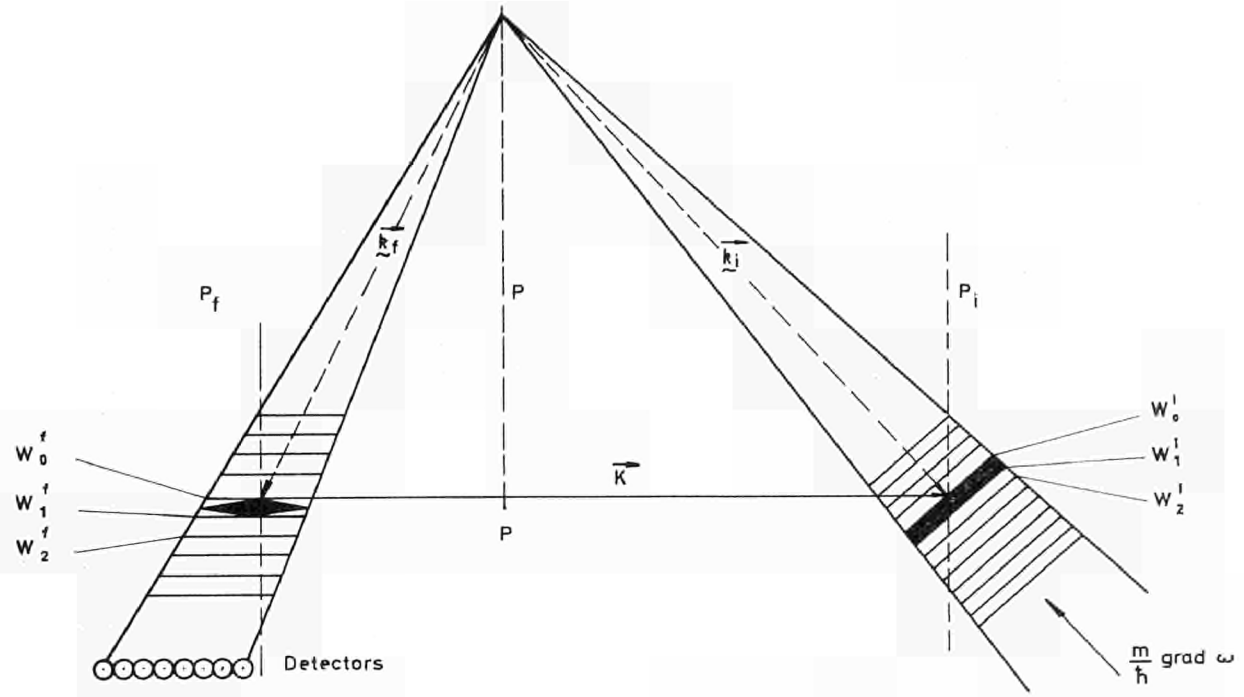

Fig. 7.a. FOCUSING CONDITION FOR TIME-OF-FLIGHT-PHONON-SPECTROSCOPY

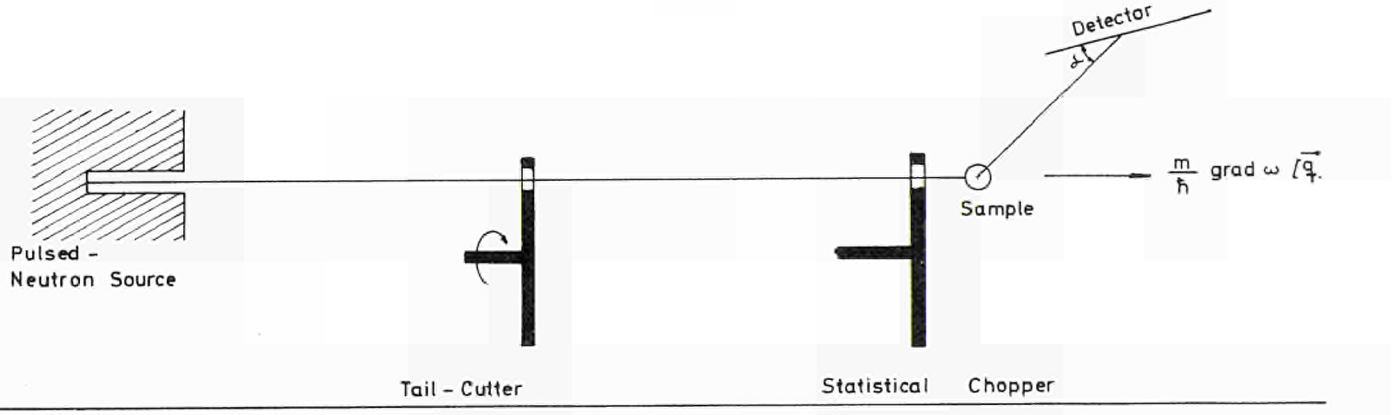

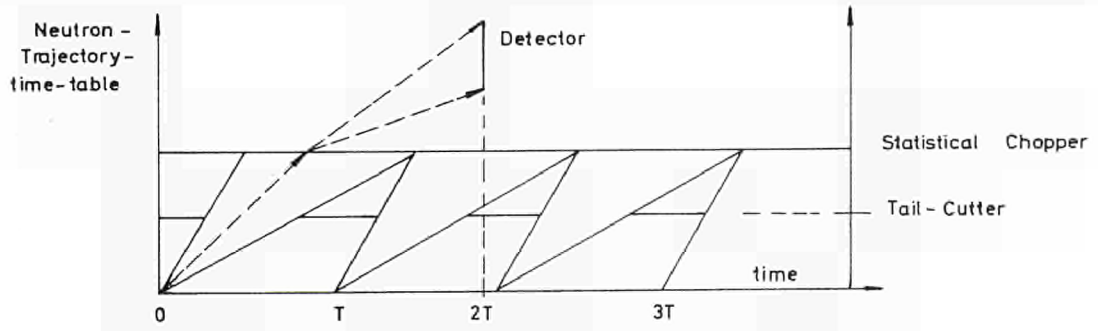

Fig. 7. b. THE MAIN FEATURES OF A TOF - EXPERIMENT IN FOCUSING CONDITION

Fig. 8.1 The mono-energetic beam, large sample spectrometer

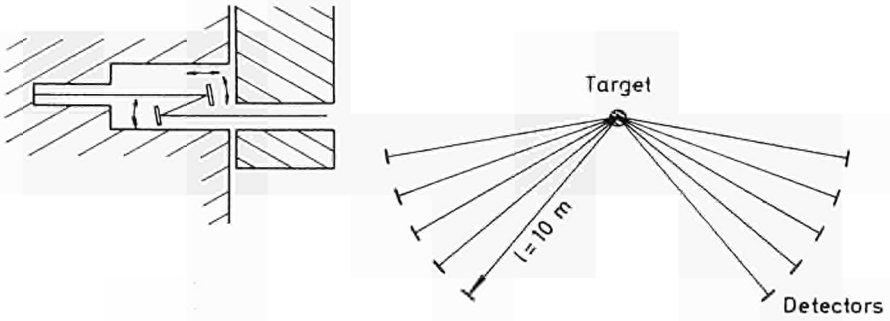

Fig. 8.2 The mono-energetic beam, small sample spectrometer

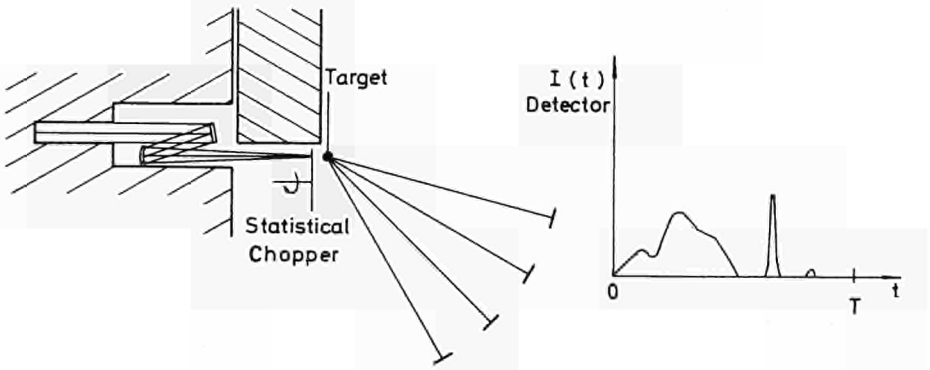

THE MONO-ENERGETIC-BEAM FACILITIES AT THE HOT, THERMAL AND COLD NEUTRON SOURCE

FIG. 8

Fig. 9.1 The general purpose white neutron beam facility of medium resolution

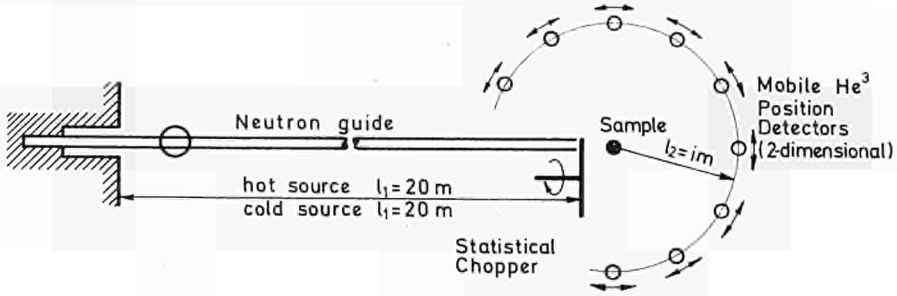

Fig. 9.2 The high resolution Laue-and Debye-Scherrer spectrometer

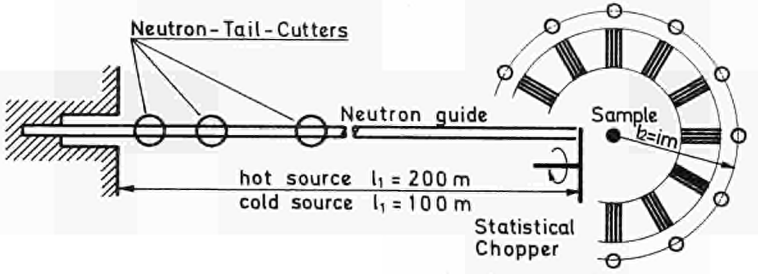

THE WHITE NEUTRON DIFFRACTION SPECTROMETERS FOR THE HOT, THERMAL AND COLD NEUTRON SOURCE

FIG. 9

Fig. 10.1 The high resolution spectrometer for coherent scattering experiments

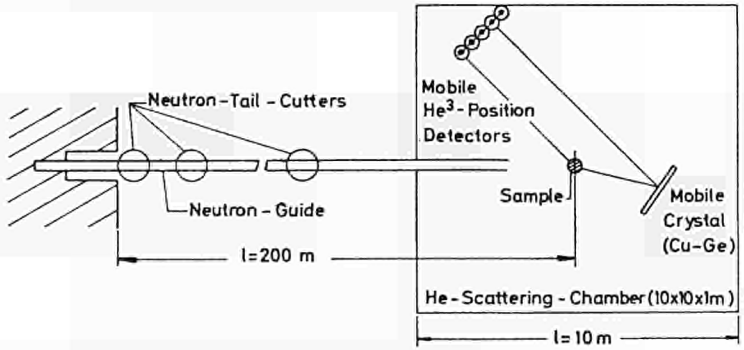

Fig. 10.2 A high resolution spectrometer for coherent scattering experiments in focusing condition

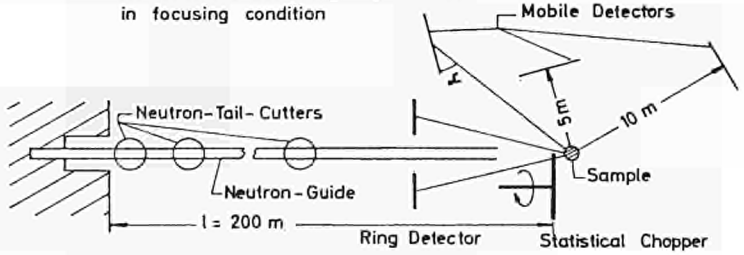

Fig. 10.3 The high resolution spectrometer for incoherent scattering experiments

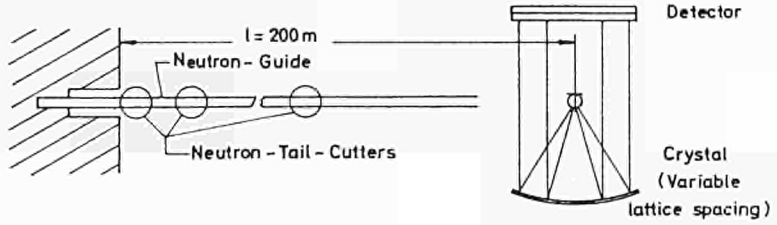

HIGH RESOLUTION SPECTROMETERS
FOR INELASTIC SCATTERING EXPERIMENTS

FIG. 10

Fig. 11.1 The inelastic small angle scattering spectrometer

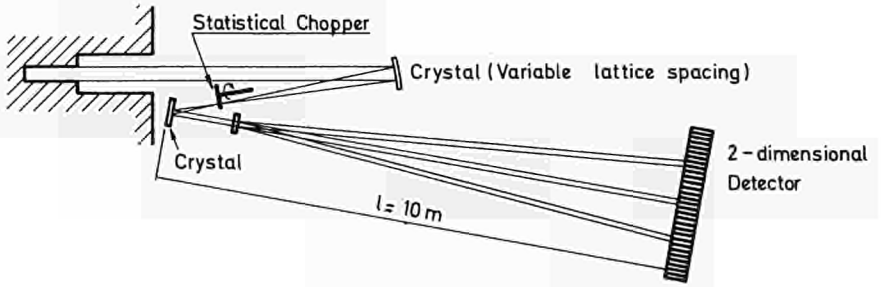

Fig. 11.2 The very cold "quasi-monochromatic" neutron beam facility

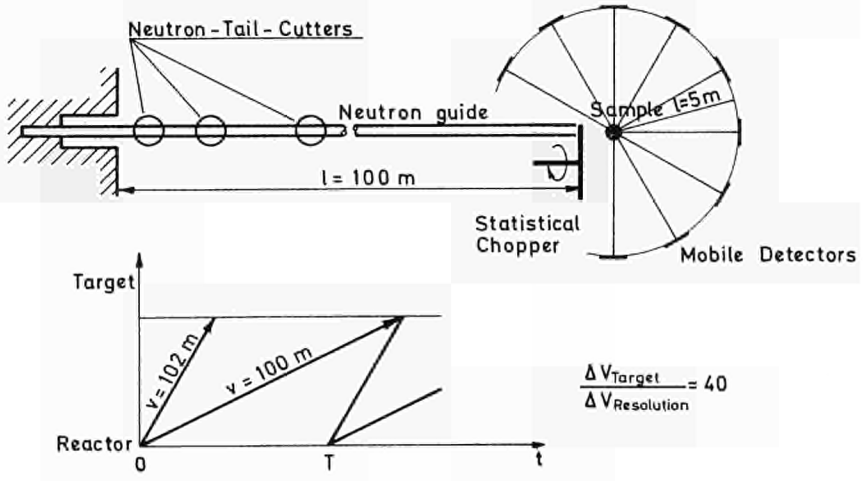

THE VERY COLD NEUTRON FACILITIES

FIG. 11

NOTICE TO THE READER

All scientific and technical reports published by the Commission of the European Communities are announced in the monthly periodical **"euro-abstracts".** For subscription (1 year: BF.1025) or free specimen copies please write to :

Office for Official Publications
of the European Communities
Boîte postale 1003
Luxembourg
(Grand-Duchy of Luxembourg)

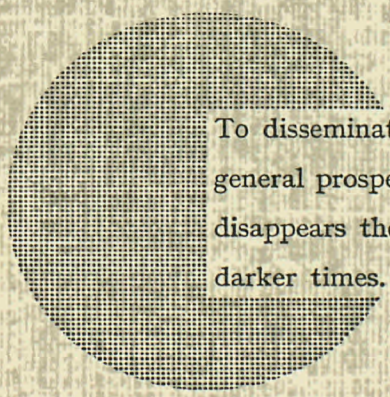

To disseminate knowledge is to disseminate prosperity — I mean general prosperity and not individual riches — and with prosperity disappears the greater part of the evil which is our heritage from darker times.

Alfred Nobel

SALES OFFICES

The Office for Official Publications sells all documents published by the Commission of the European Communities at the addresses listed below, at the price given on cover. When ordering, specify clearly the exact reference and the title of the document.

UNITED KINGDOM

H.M. Stationery Office
P.O. Box 569
London S.E. 1 — Tel. 01-928 69 77, ext. 365

BELGIUM

Moniteur belge — Belgisch Staatsblad
Rue de Louvain 40-42 — Leuvenseweg 40-42
1000 Bruxelles — 1000 Brussel — Tel. 12 00 26
CCP 50-80 — Postgiro 50-80

Agency :
Librairie européenne — Europese Boekhandel
Rue de la Loi 244 — Wetstraat 244
1040 Bruxelles — 1040 Brussel

DENMARK

J.H. Schultz — Boghandel
Møntergade 19
DK 1116 København K — Tel. 14 11 95

FRANCE

Service de vente en France des publications des Communautés européennes — Journal officiel
26, rue Desaix — 75 732 Paris - Cédex 15e
Tel. (1) 306 51 00 — CCP Paris 23-96

GERMANY (FR)

Verlag Bundesanzeiger
5 Köln 1 — Postfach 108 006
Tel. (0221) 21 03 48
Telex: Anzeiger Bonn 08 882 595
Postscheckkonto 834 00 Köln

GRAND DUCHY OF LUXEMBOURG

Office for Official Publications of the European Communities
Boîte postale 1003 — Luxembourg
Tel. 4 79 41 — CCP 191-90
Compte courant bancaire: BIL 8-109/6003/200

IRELAND

Stationery Office — The Controller
Beggar's Bush
Dublin 4 — Tel. 6 54 01

ITALY

Libreria dello Stato
Piazza G. Verdi 10
00198 Roma — Tel. (6) 85 08
CCP 1/2640

NETHERLANDS

Staatsdrukkerij- en uitgeverijbedrijf
Christoffel Plantijnstraat
's-Gravenhage — Tel. (070) 81 45 11
Postgiro 42 53 00

UNITED STATES OF AMERICA

European Community Information Service
2100 M Street, N.W.
Suite 707
Washington, D.C., 20 037 — Tel. 296 51 31

SWITZERLAND

Librairie Payot
6, rue Grenus
1211 Genève — Tel. 31 89 50
CCP 12-236 Genève

SWEDEN

Librairie C.E. Fritze
2, Fredsgatan
Stockholm 16
Post Giro 193, Bank Giro 73/4015

SPAIN

Libreria Mundi-Prensa
Castello 37
Madrid 1 — Tel. 275 51 31

OTHER COUNTRIES

Office for Official Publications of the European Communities
Boîte postale 1003 — Luxembourg
Tel. 4 79 41 — CCP 191-90
Compte courant bancaire: BIL 8-109/6003/200

OFFICE FOR OFFICIAL PUBLICATIONS OF THE EUROPEAN COMMUNITIES
Boîte postale 1003 — Luxembourg 6293

CDNA05046ENC